



# Dynamics of Nonlinear Interactions between Electron Temperature Gradient Mode and Ion-scale Fluctuations in Linear Magnetized Plasmas

**Chанho Moon<sup>1,2</sup>, Toshiro Kaneko<sup>2</sup>, Rikizo Hatakeyama<sup>2</sup>,  
Tatsuya Kobayashi<sup>1</sup>, Kimitaka Itoh<sup>1</sup>**

<sup>1</sup>*National Institute for Fusion Science, 322-6 Oroshi-cho, Toki-shi, 509-5292, Japan*

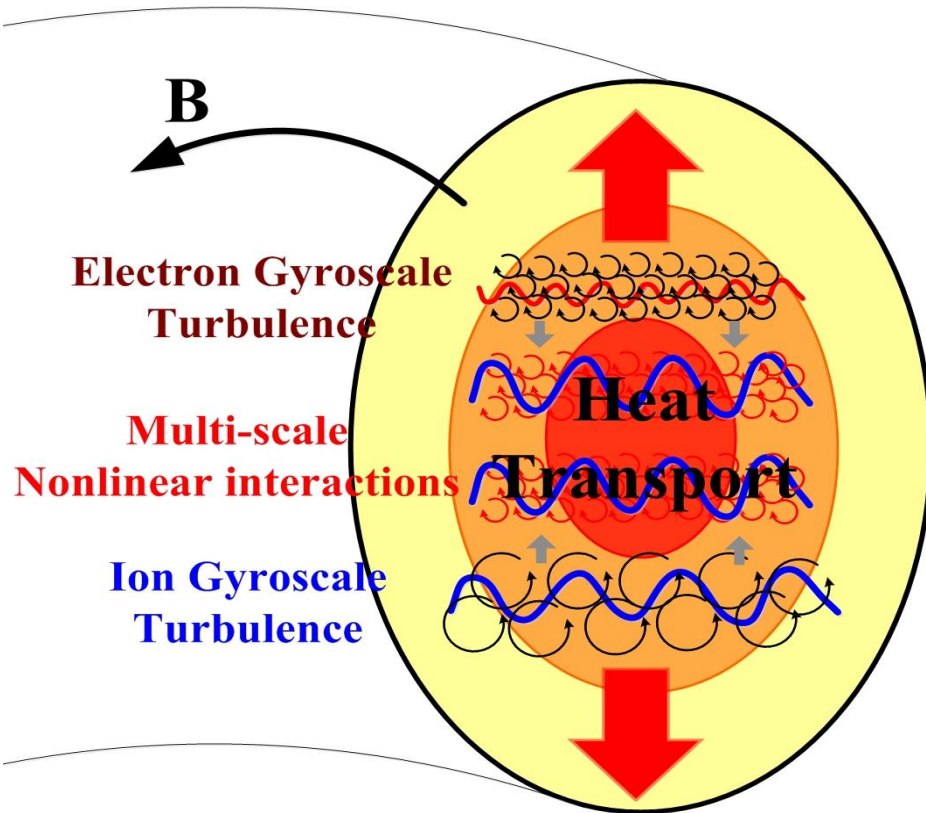
<sup>2</sup>*Department of Electronic Engineering, Tohoku University, Sendai 980-8579, Japan*

E-mail : *moon.chanho@LHD.nifs.ac.jp*

# Outline

- 1. Background and Purpose**
- 2. Experimental Apparatus**
- 3. Experimental Results**
- 4. Summary**

# Background and Purpose



- Open problems on ETG mode
- Excitation mechanism
- Suppression mechanism

1) W. Horton, Rev. Mod. Phys. **71** (1999) 735.

2) F. Brochard et al., Phys. Plasmas **12** (2005) 062104.

3) V. Sokolov et al., Phys. Rev. Lett. **89** (2002) 095001.

4) S. K. Mattoo et al., Phys. Rev. Lett. **108** (2012) 255007.

## Anomalous heat transport —ion scale—

### Gradient Driven Instability

- Drift wave (DW) mode<sup>1)</sup>
- Flute mode<sup>2)</sup>
- Ion temperature gradient (ITG) mode<sup>3)</sup>

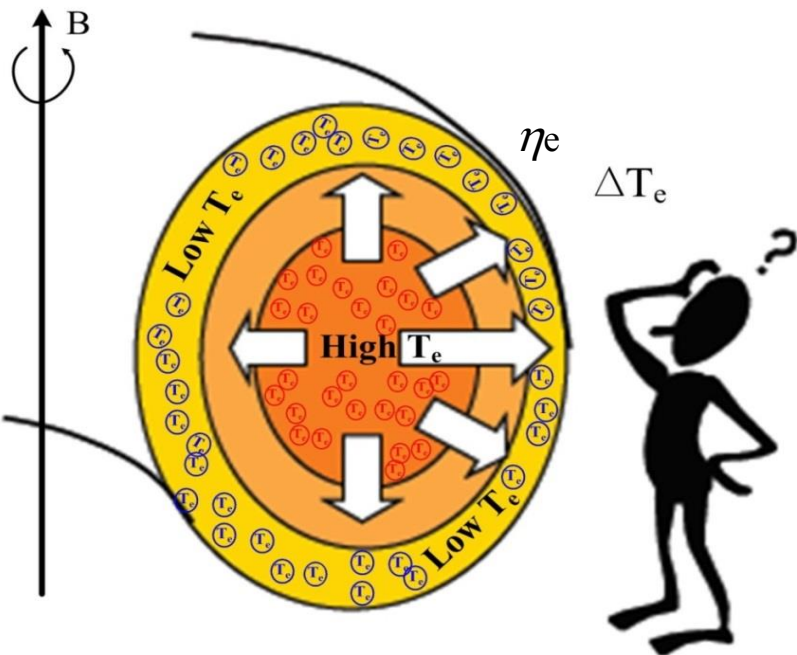
### Anomalous electron heat transport

### Electron Temperature Gradient (ETG) Mode<sup>4)</sup>

$$\text{electron heat transport} \sim (\chi_e \sim \chi_i) \quad \text{ion heat transport}$$

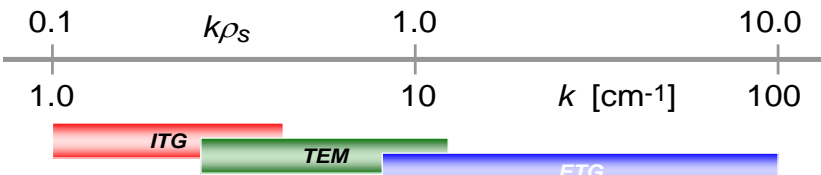
Produce and control the ETG  
to understand the mechanism of  
excitation and multi-scale  
interaction of the ETG mode

# Research of ETG mode



## ETG mode:

- Electrostatic mode (low  $\beta$ )
- Electron diamagnetic direction
- $k_{\perp} \rho_e \leq 1 < k_{\perp} \rho_i$ ,  $\Omega_i < \omega \ll \Omega_e$



Wavelength scales of Fluctuations

## Theory

### ✓ Excitation

- Y. C. Lee et al., Phys. Fluids **30**, 1331 (1987).
- W. Horton and B. G. Hong, Phys. Fluids **31**, 2971 (1988).
- Y. Idomura et al., Phys. Plasmas **7**, 2456 (2000).
- W. Dorland et al., Phys. Rev. Lett. **85**, 5579 (2000).
- S.-I. Itoh and K. Itoh, Plasma Phys. Control. Fusion **43**, 1055 (2001).
- F. Jenko, J. Plasma Fusion Res. Ser. **6**, 11 (2004).

### ✓ Suppression

### Multi-Scale Interactions

- Z. Gao et al., Phys. Plasmas **11**, 3053 (2004).
- M. Romanelli et al., Phys. Plasmas **11**, 3845 (2004).

## Experiment

### ✓ Excitation

- E. Mazzucato et al., Phys. Rev. Lett. **101**, 075001 (2008).  
→ Observation
- X. Wei et al., Phys. Plasmas **17**, 042108 (2010).  
→ Identification
- X. R. Fu et al., Phys. Rev. Lett. **19**, 032303 (2012).  
→ High  $\beta$

### ✓ Suppression

- D. R. Smith et al., Phys. Rev. Lett. **102**, 225005 (2009).  
→ Large  $E \times B$  Shear
- H. Y. Yuh et al., Phys. Rev. Lett. **106**, 055003 (2011).  
→ Magnetic Shear

# $\nabla$ -Driven Instability / Turbulence

	Excitation 'Bare' Instability	Multi-Scale Interaction	Suppression
Ion-scale $\sim \rho_i$	<ul style="list-style-type: none"> <li>• Drift wave ~ 1960</li> <li>• Geometrical ~ 1980 (<math>\nabla B</math>, ...)</li> <li>• Trapped particle</li> <li>• ITG mode ~ 1990</li> </ul>	<ul style="list-style-type: none"> <li>• Geodesic acoustic mode (Conway, Nagashima)</li> <li>• Zonal flow (Fujisawa, ...)</li> <li>• Streamer (Yamada, ...)</li> </ul> <p>※Causal relations “Multi-scale Renormalized Turbulence”</p>	<ul style="list-style-type: none"> <li>• <math>E \times B</math> flow shear</li> <li>• linear or nonlinear</li> </ul>
Electron-scale $\sim \rho_e$	<p>※ Experi.</p> <ul style="list-style-type: none"> <li>✓ <u>ETG mode</u></li> <li>• Observation (E. Mazzucato) ~ 2008</li> <li>• Identification (X. Wei) ~ 2010</li> <li>• High <math>\beta</math> (X. R. Fu) ~ 2012</li> </ul>		<ul style="list-style-type: none"> <li>• Large <math>E \times B</math> shear (D. R. Smith)</li> <li>• Magnetic Shear (H. Y. Yuh)</li> <li>• Density Gradient (Y. Ren)</li> </ul>
	<p>※ Theories</p> <ul style="list-style-type: none"> <li>✓ <u>ETG mode</u> (Horton, Dorland, Jenko, ....) ~ 1990</li> </ul>	<ul style="list-style-type: none"> <li>• Elongated toroidal (cascade, Jenko)</li> <li>• Nonlinear ion-scale DW (radially elongated, Itoh, Jenko)</li> <li>• Streamer (Idomura)</li> <li>• Zonal flow (?) feeble (Diamond)</li> </ul>	<ul style="list-style-type: none"> <li>• <math>E \times B</math> shear (Z. Gao)</li> </ul>

# Experimental Apparatus for ETG Mode

## National Spherical Torus Experiment (NSTX)

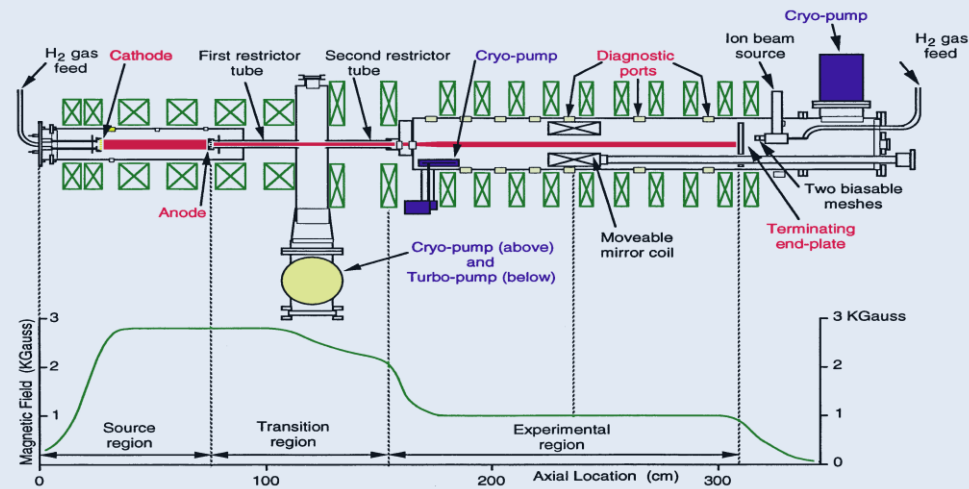


Fluctuations :  $\omega/2\pi \sim 1$  MHz  
 $T_e = \sim 2$  keV,  $n_e = \sim 4 \times 10^{19} \text{ m}^{-3}$

- Troidal Device
- Difficult to Control ETG
- Changing Plasma Parameters

## Columbia Linear Machine (CLM)

### Columbia Linear Machine



Fluctuations:  $\omega/2\pi \sim 2$  MHz  
 $T_e = 5-15$  eV,  $n_e = \sim 2 \times 10^{15} \text{ m}^{-3}$

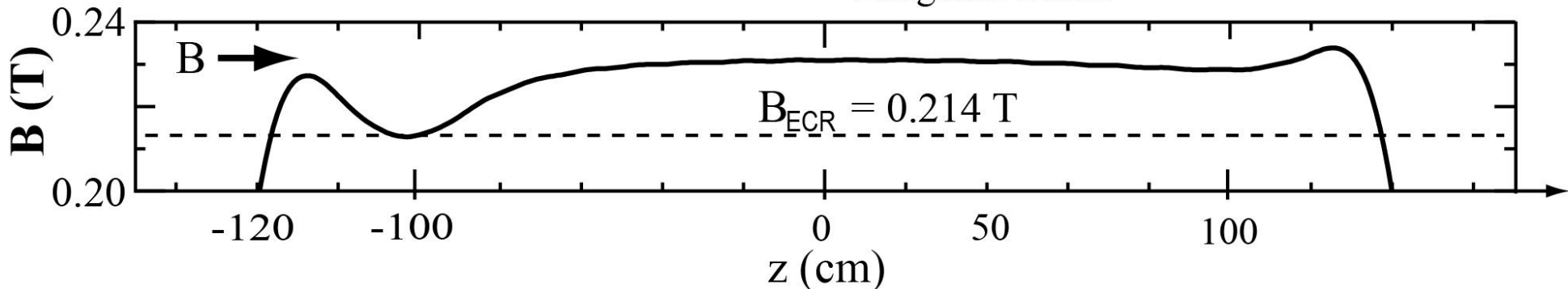
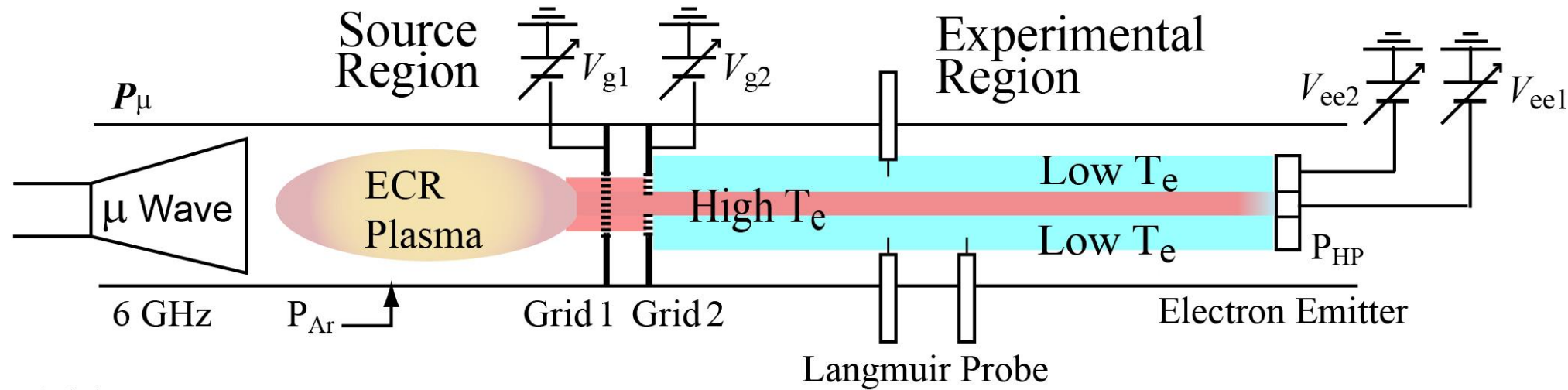
- Linear Device
- Using the Electron Beam
- Forming the Density Gradient

# Experimental Apparatus

$P_\mu = 20 \text{ W}$   
 $P_{HP} = 3 \text{ kW}$   
 $P_{Ar} = 1 \times 10^{-4} \text{ Torr}$

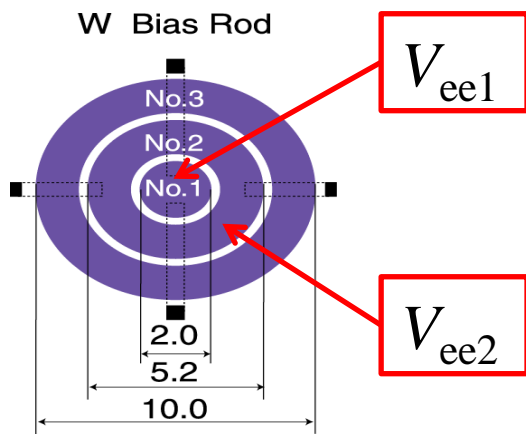
10 mesh/inch      30 mesh/inch

$B : 0.214 \sim 0.23 \text{ T}$   
 $\rho_e = \sim 0.04 \text{ mm}, \rho_i = \sim 2.5 \text{ mm}$

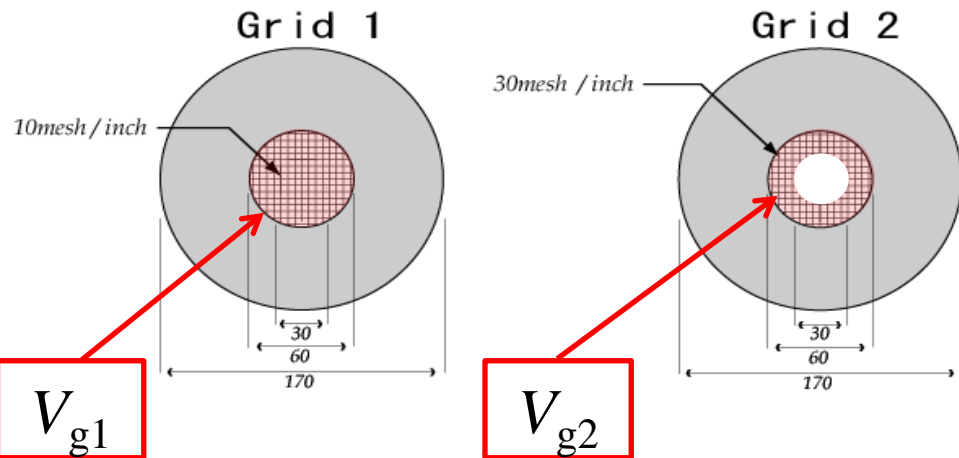


Q<sub>T</sub> Upgrade Machine at Tohoku University

## Electron emitter (W hot plate)

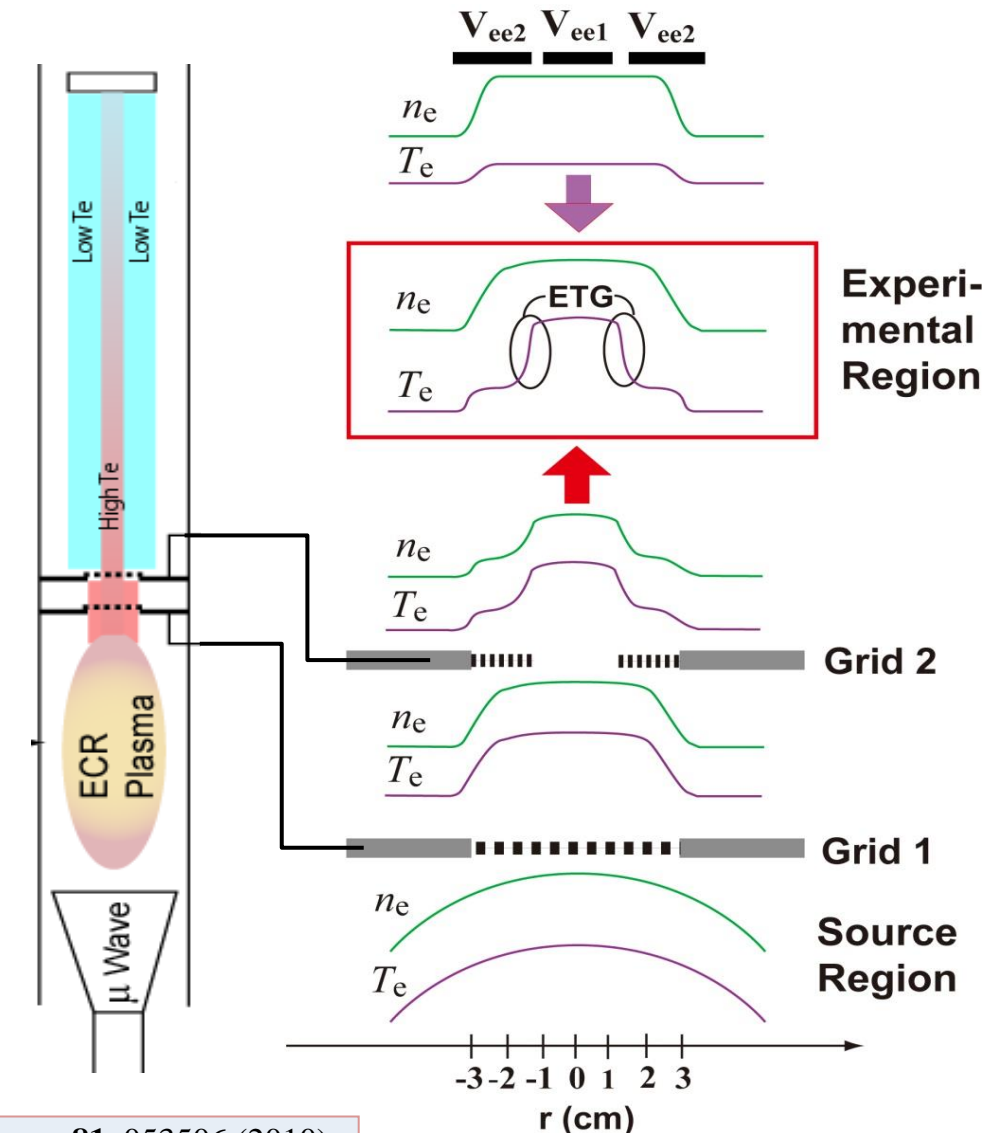


## Configuration of mesh grids



## Electron emitter

8



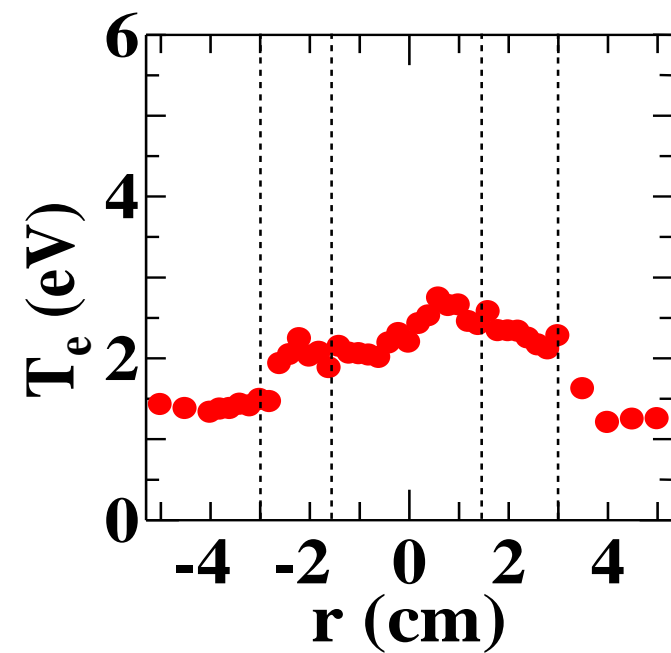
C. Moon, T. Kaneko, S. Tamura, and R. Hatakeyama, Rev. Sci. Instrum. **81**, 053506 (2010).

**Control of the electron density and temperature profiles from the source to experimental regions by using the mesh grids.**

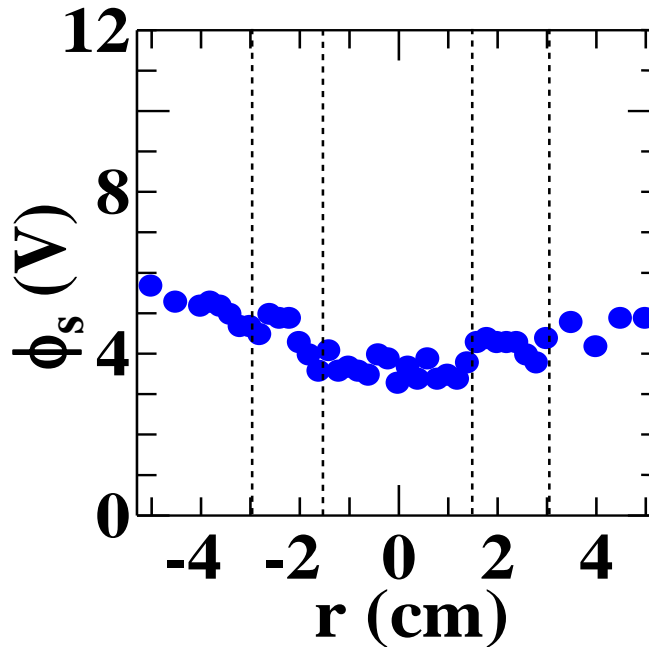
# Plasma Parameters

$$\begin{aligned}
 P_{\mu} &= 60 \text{ W}, \quad P_{HP} = 3 \text{ kW}, \quad P_{Ar} = 1 \times 10^{-4} \text{ Torr} \\
 V_{g1} &= 0 \text{ V}, \quad V_{g2} = 0 \text{ V}, \quad V_{ee1} = 0 \text{ V}, \quad V_{ee2} = 0 \text{ V}
 \end{aligned}$$

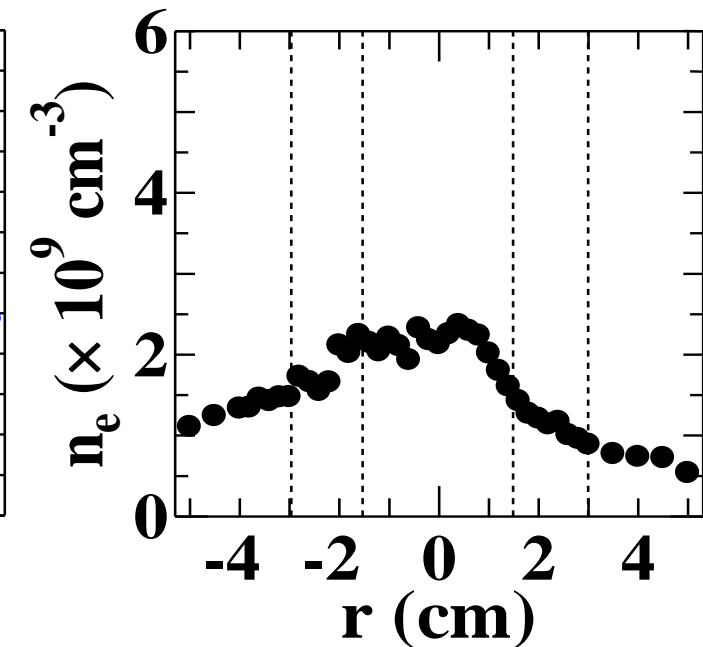
**Electron Temperature**



**Space Potential**



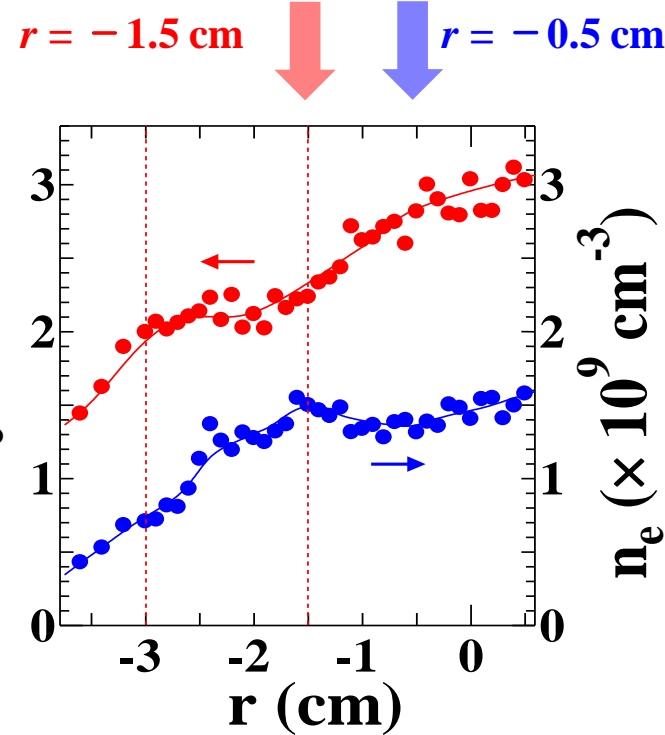
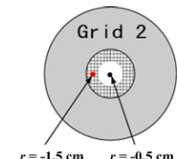
**Electron Density**



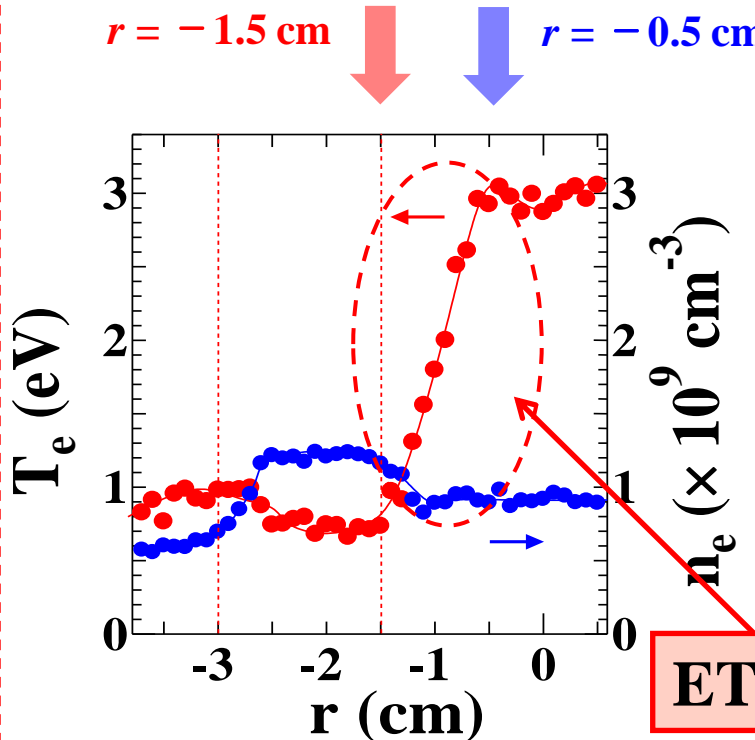
**Radial Profiles of a Typical Plasma Parameters**

# Formation and Control of ETG

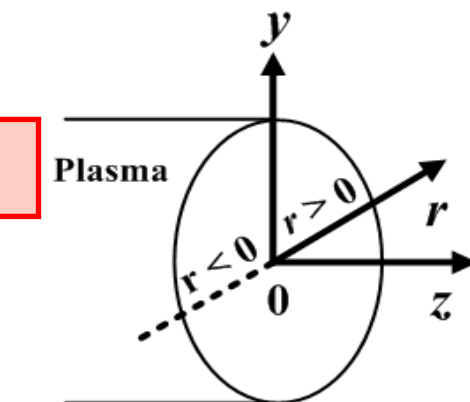
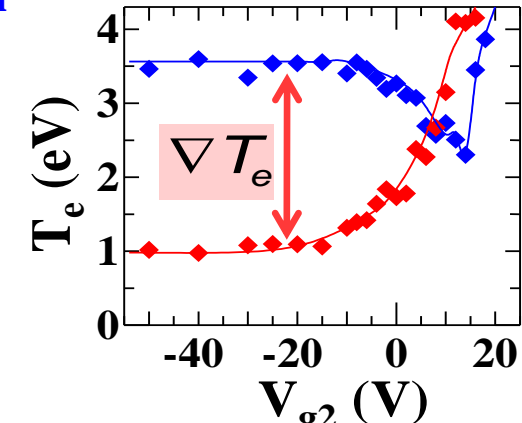
$$P_{\mu} = 20 \text{ W}, V_{ee1} = -4 \text{ V}, V_{ee2} = -1.5 \text{ V}, V_{g1} = -10 \text{ V}$$



$$V_{g2} = 3 \text{ V}$$



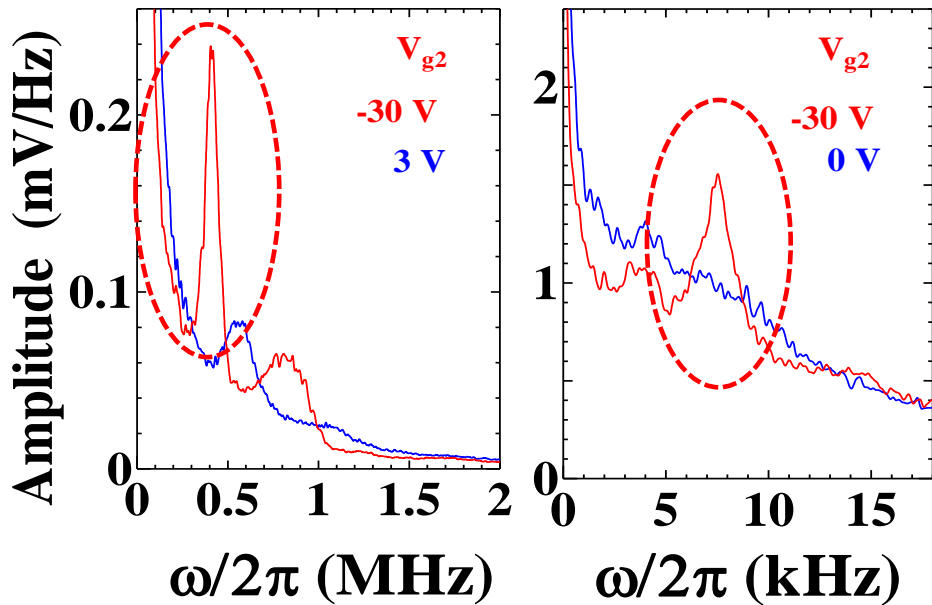
$$V_{g2} = -30 \text{ V}$$



ETG can be generated easily by controlling the grid bias voltages  $V_{g2}$ .

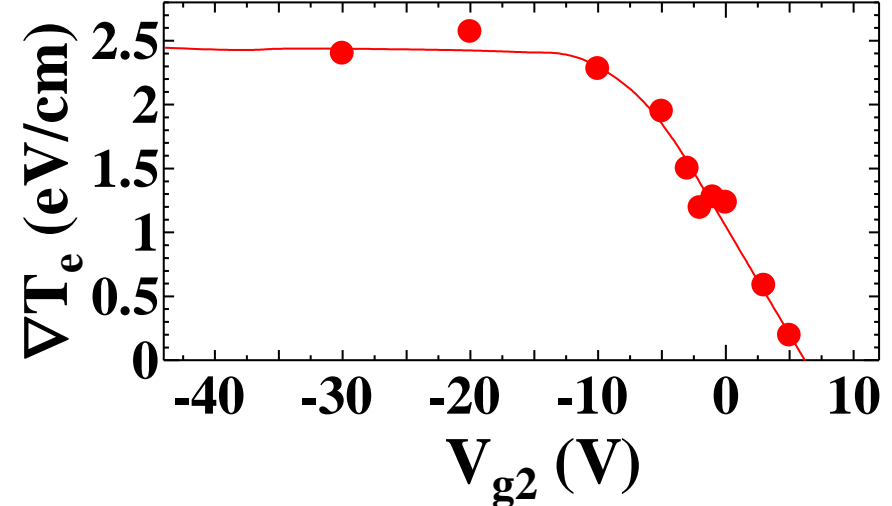
# Effect of ETG on Fluctuations

$$\begin{aligned}
 P_\mu &= 20 \text{ W}, V_{ee1} = -4 \text{ V} \\
 V_{ee2} &= -1.5 \text{ V}, V_{g1} = -10 \text{ V} \\
 r &= -1.5 \text{ cm}
 \end{aligned}$$

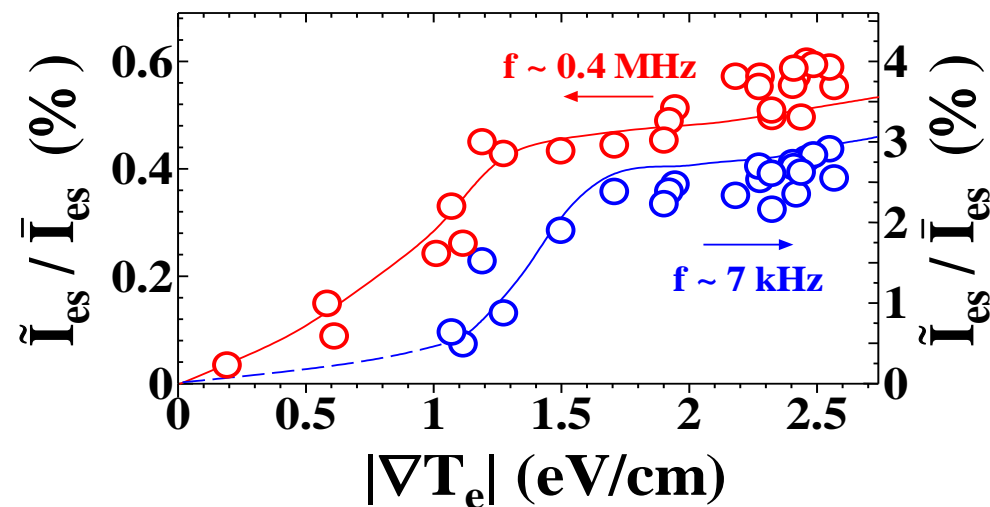


high and low frequency

ETG ( $\nabla T_e$ )



Normalized Amp.



A high-frequency fluctuation ( $\sim 0.4$  MHz) is excited in situations where large ETG is formed (ETG mode).

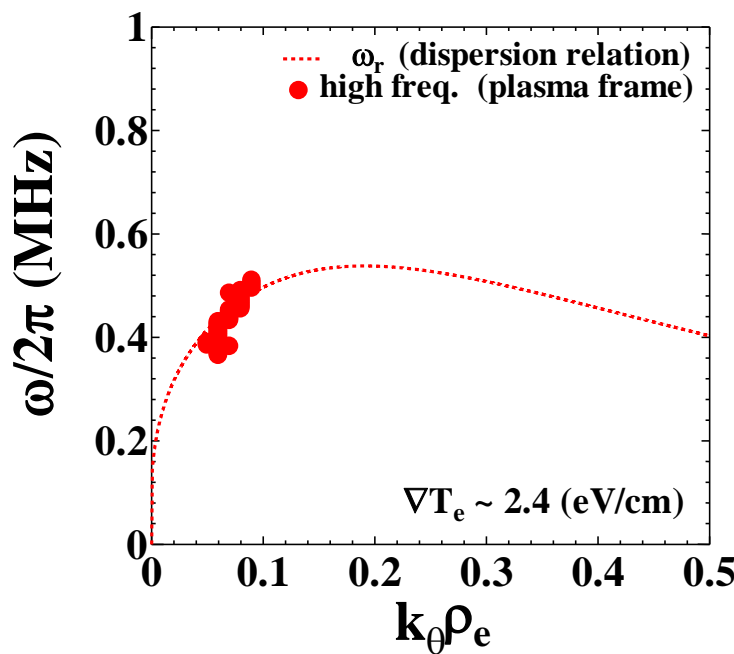
# Linear Dispersion Relations

The perturbed electron density of the linearized Vlasov equation:

$$\tau + (k_{\perp} \lambda_{De})^2 + b \left( 1 + \frac{1}{2\lambda_e^2} \right) - \frac{1}{2\lambda_e^2} + b \frac{\omega_{T_e}^*}{\omega} + \frac{\omega_{T_e}^*}{4\lambda_e^2 \omega} (1+b) = 0,$$

where  $\tau = \frac{T_e}{T_i}$ ,  $k_{\perp} = k_y$ ,  $\lambda_e = \frac{\omega}{k_{\parallel} v_e}$ ,  $b = \frac{(k_{\perp} \rho_e)^2}{2}$ ,  $\omega_{T_e}^* = \frac{k_{\perp} T_e}{e B L_{T_e}}$ .

[Phys. Fluids **30**, 1331 (1987), Phys. Plasmas **17**, 042108 (2010)]



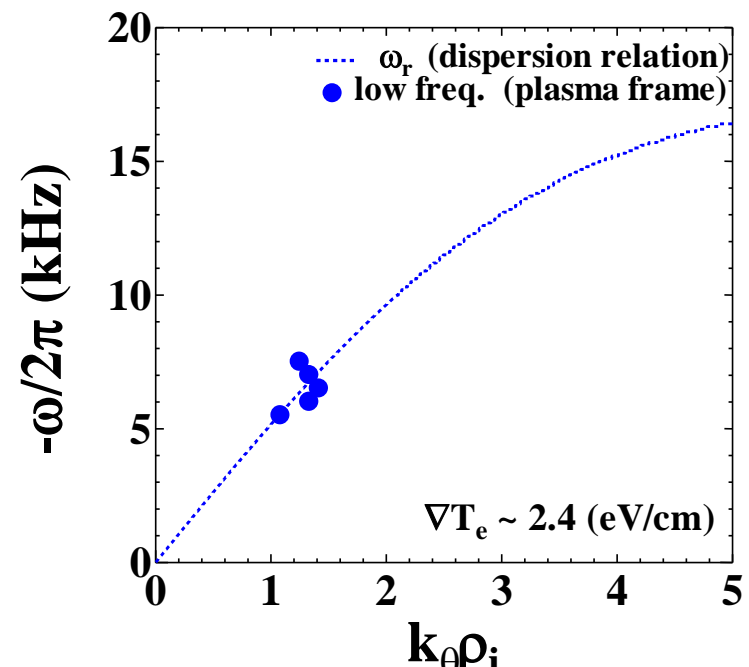
**ETG mode (~ 0.4MHz)**

The typical experimental plasma parameters

$$T_{e0} = 3 \text{ eV}, T_i = 0.3 \text{ eV}, n_e = 1 \times 10^9 \text{ cm}^{-3},$$

$$\lambda_{De} = 0.039 \text{ cm}, B = 2300 \text{ G}, L_{T_e} = 1.2 \text{ cm},$$

$$k_{\parallel} = 0.06 \text{ cm}^{-1}, \rho_e = 0.004 \text{ cm}, \rho_i = 0.25 \text{ cm}.$$



**DW mode (~7 kHz)**

The high and low frequency of fluctuations are consistent with the theoretical estimation from the linear dispersion relation of ETG and DW

# Bispectral Analysis (Nonlinear Coupling)

**Bicoherence:** the degree of nonlinear coupling between the three waves (the value in the range from 0 to 1)

The bicoherence is defined as

$$b_{xyz}^2(f_1, f_2) = \frac{\left| \langle B_{xyz}(f_1, f_2) \rangle \right|^2}{\langle |X(f_1 + f_2)|^2 \rangle \langle |Y(f_1)Z(f_2)|^2 \rangle}$$

<>: Averaged ensembles

- The variance of the bicoherence is  $d b^2(f_1 + f_2) \leq 1/N \sim 0.0014$ .

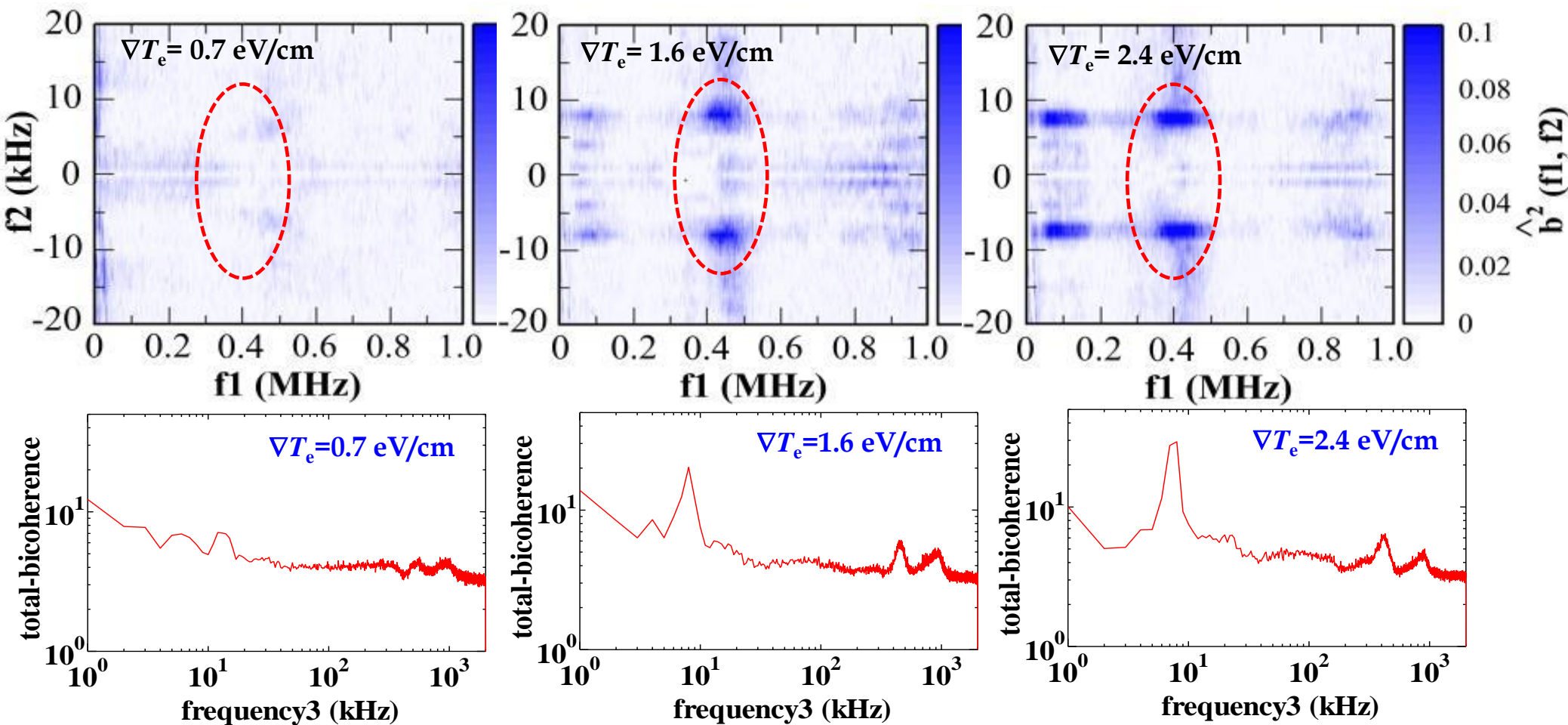
The bispectral analysis can clarify the three-wave nonlinear interactions quantitatively.

# Bicoherence of the High & Low Frequency Fluctuations

14

## Squared Bicoherence

$$P_\mu = 20 \text{ W}, V_{g1} = -10 \text{ V}, V_{ee1} = -4.0 \text{ V}, \\ V_{ee2} = -1.5 \text{ V}, r = -1.5 \text{ cm}$$



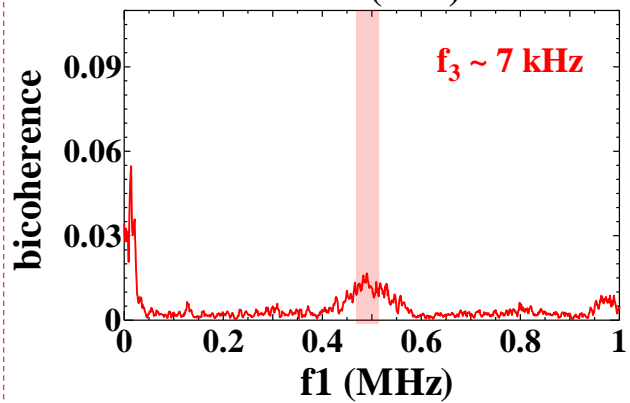
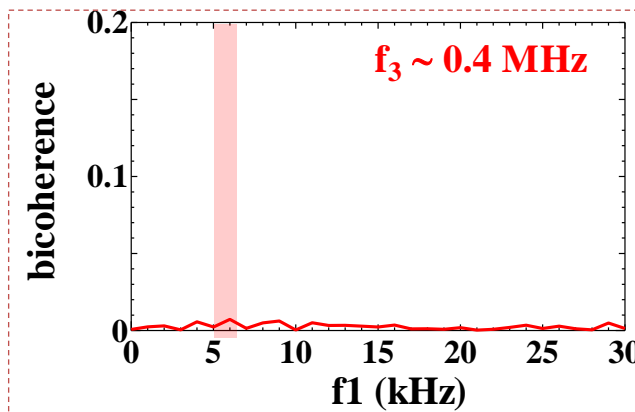
The nonlinear coupling between the ETG mode and drift wave (DW) mode become stronger as the magnitude of ETG is increased.

# Bicoherence of the High & Low Frequency Fluctuations

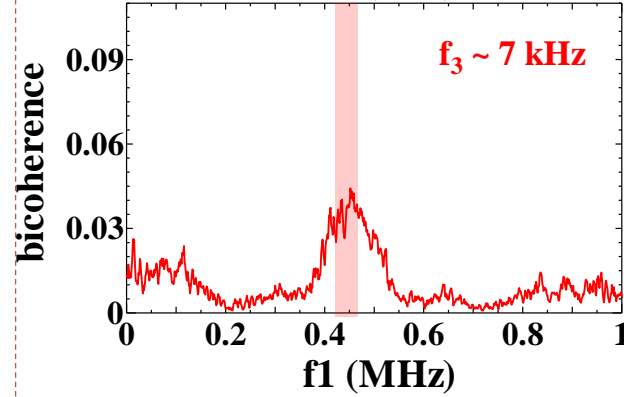
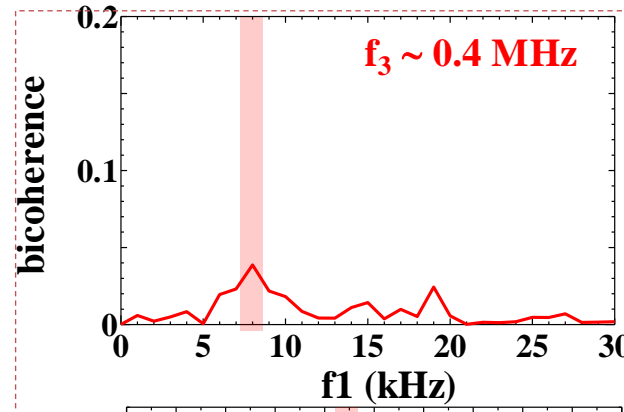
15

**ETG (~0.4 MHz) & DW (~7 kHz) modes**

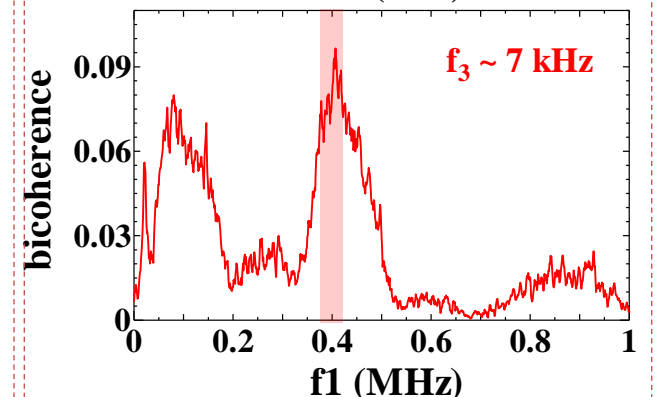
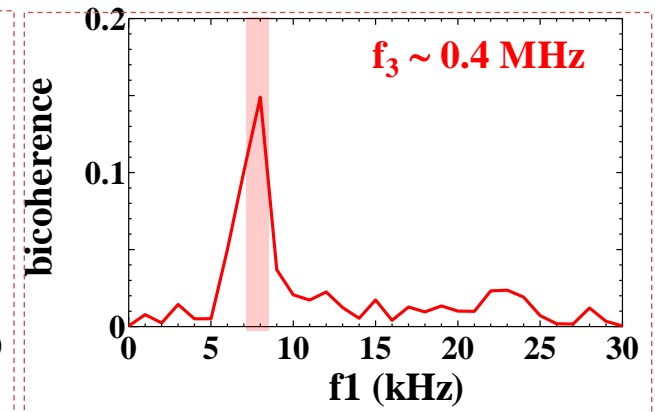
$$P_{\mu} = 20 \text{ W}, V_{g1} = -10 \text{ V}, V_{ee1} = -4.0 \text{ V}, \\ V_{ee2} = -1.5 \text{ V}, r = -1.5 \text{ cm}$$



$$\nabla T_e = 0.7 \text{ eV/cm}$$



$$\nabla T_e = 1.6 \text{ eV/cm}$$



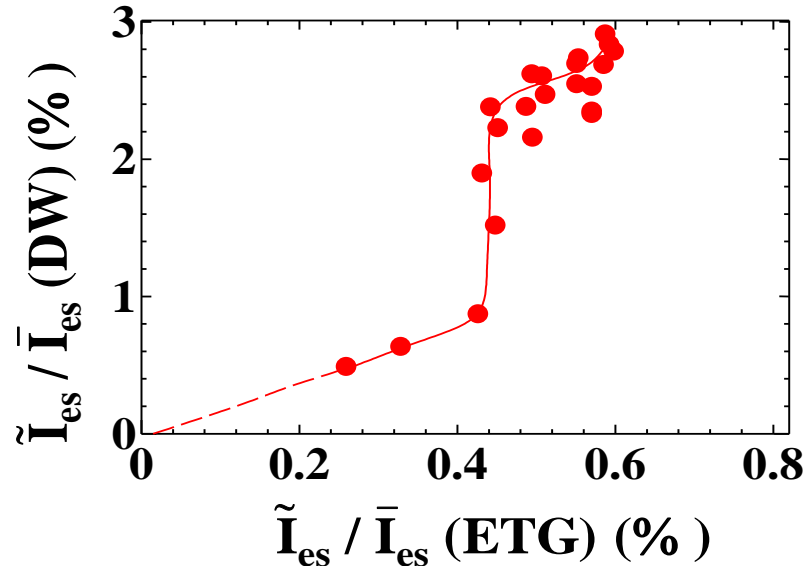
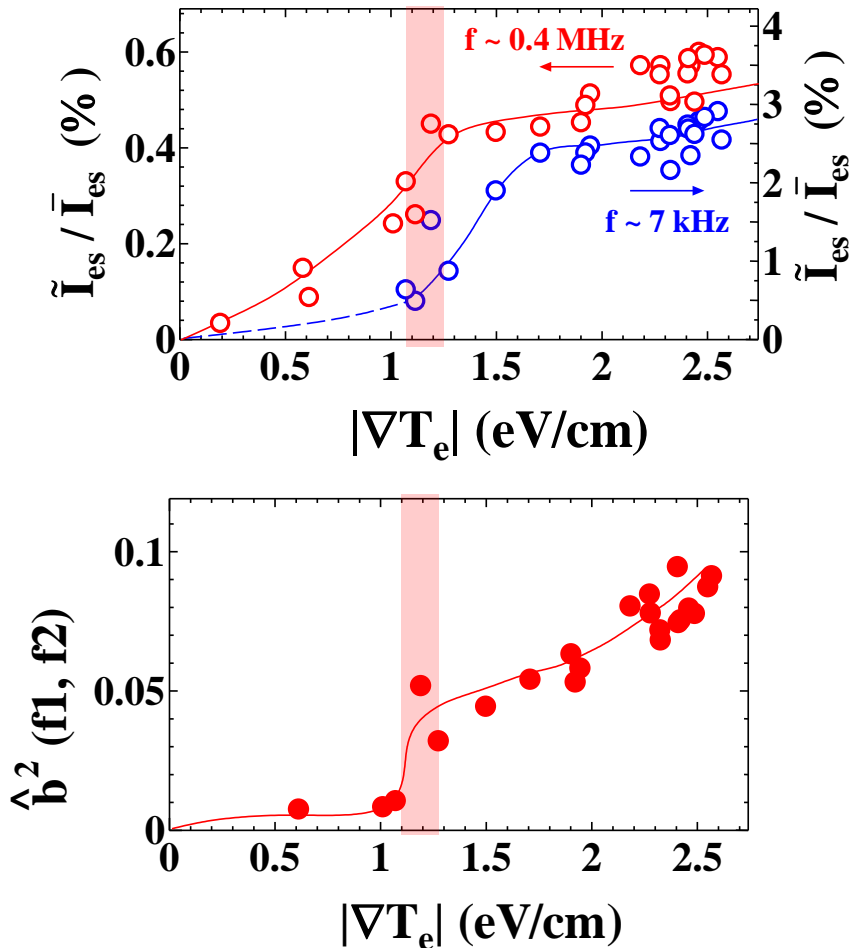
$$\nabla T_e = 2.4 \text{ eV/cm}$$

When the magnitude of ETG is increased, the slice of bicoherence between ETG mode and drift wave mode has a noticeable peak.

# Nonlinear Energy Transfer (drift wave mode)

16

$$P_\mu = 20 \text{ W}, V_{g1} = -10 \text{ V}, V_{ee1} = -4 \text{ V}, V_{ee2} = -1.5 \text{ V}, r = -1.5 \text{ cm}$$



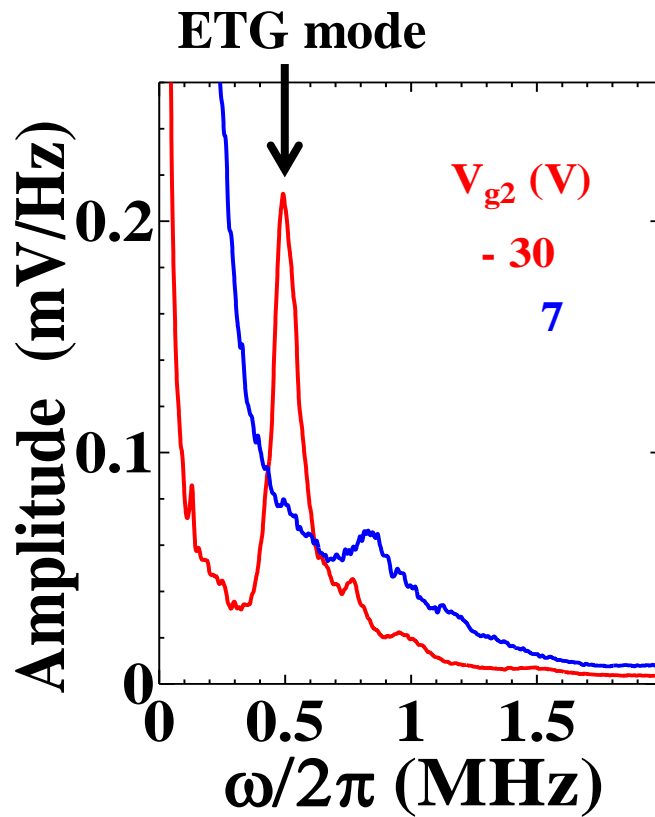
※ High-frequency fluctuations (ETG mode) versus low-frequency fluctuations (Drift wave mode).

C. Moon, T. Kaneko, and R. Hatakeyama,  
*Phys. Rev. Lett.* **111**, 115001 (2013).

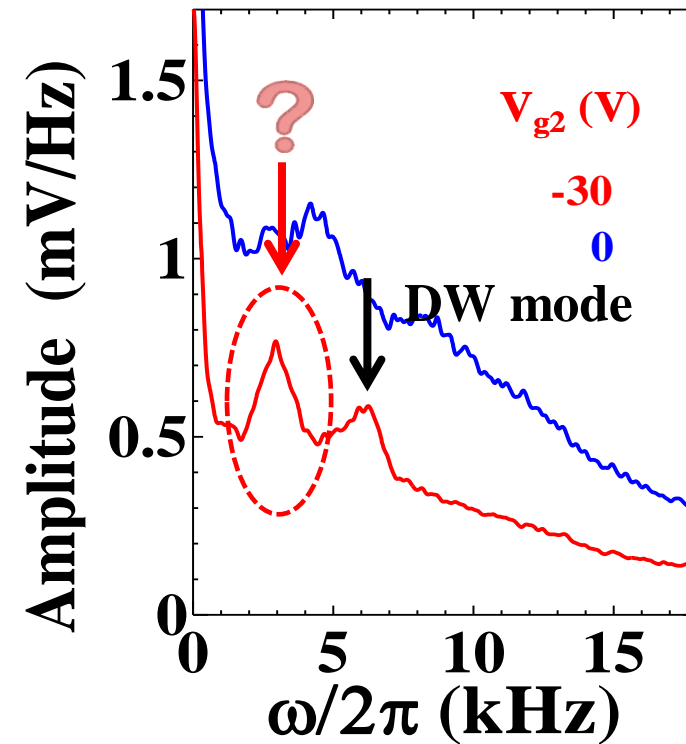
The energy of the ETG mode is transferred to the drift wave mode through the nonlinear interaction for  $\nabla T_e \geq 1.2 \text{ eV/cm}$ .

# Effect of ETG on Fluctuations

$$P_{\mu} = 20 \text{ W}, V_{ee1} = -4 \text{ V}, V_{ee2} = -1.5 \text{ V}, V_{g1} = -10 \text{ V}, r = -0.9 \text{ cm}$$



High-Frequency

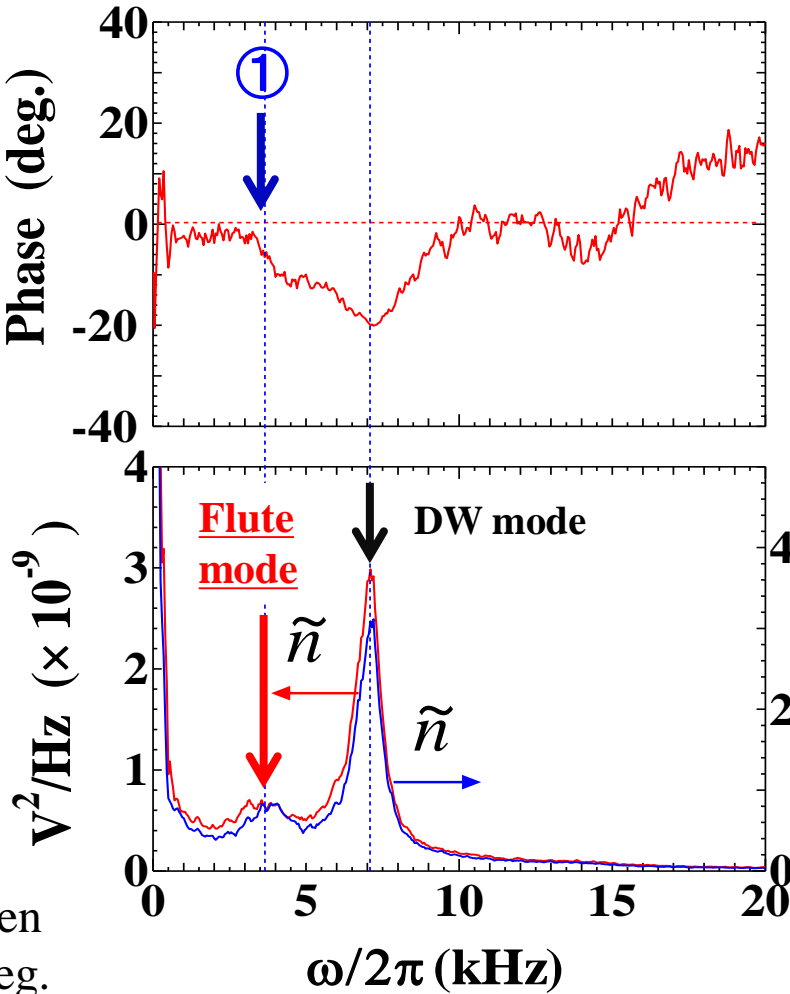
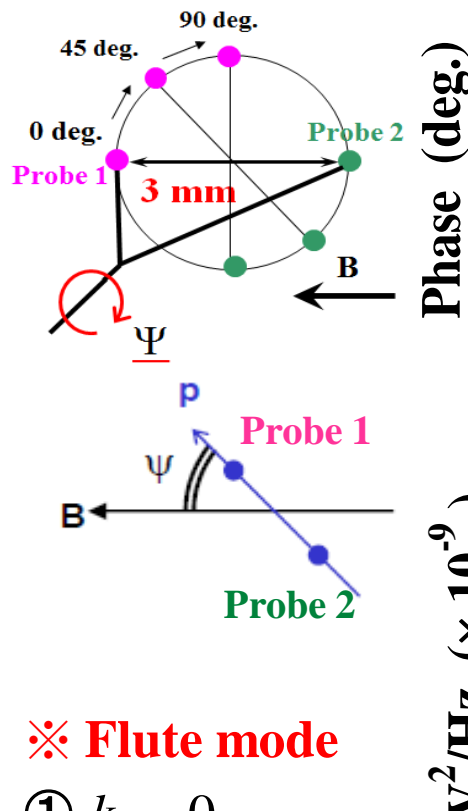


Low-Frequency

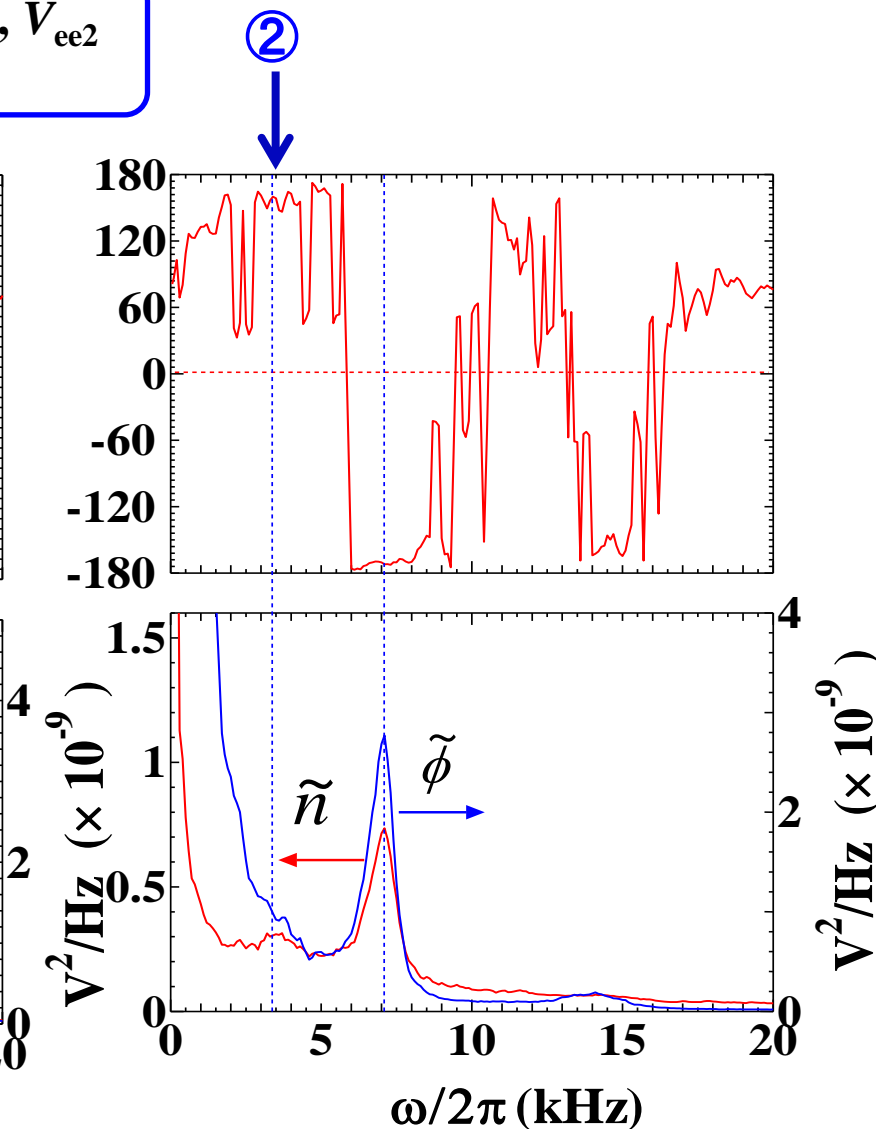
It is observed another low-frequency ( $\sim 3.6$  kHz) mode when the large ETG is formed.

# Identification of a low-frequency fluctuation

$$P_\mu = 20 \text{ W}, V_{g1} = -10 \text{ V}, V_{g2} = -30 \text{ V}, V_{ee1} = -4.0 \text{ V}, V_{ee2} = -1.5 \text{ V}, r = 1.5 \text{ cm}, \Psi \sim 0^\circ$$



Phase shift between  $\tilde{n}$  and  $\tilde{n}$

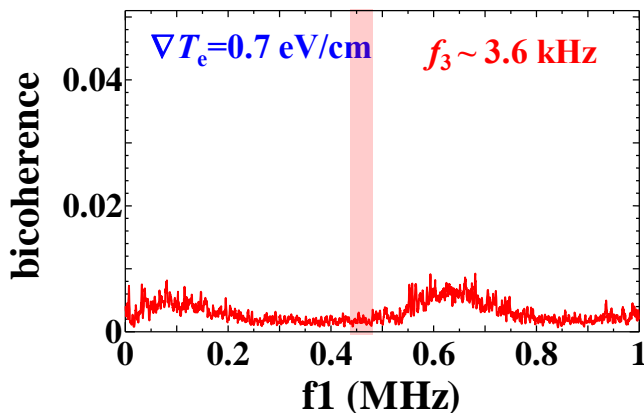


Phase shift between  $\tilde{n}$  and  $\tilde{\phi}$

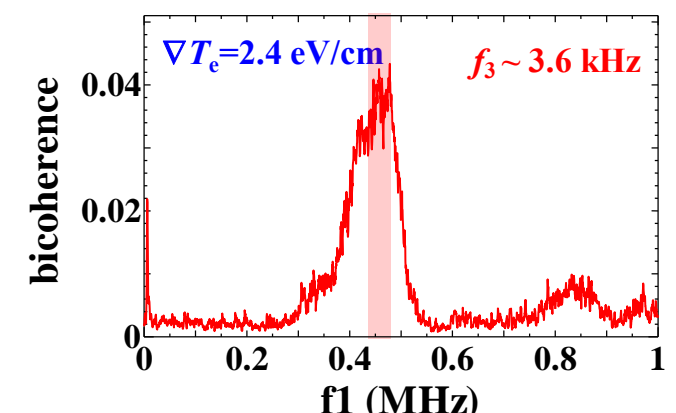
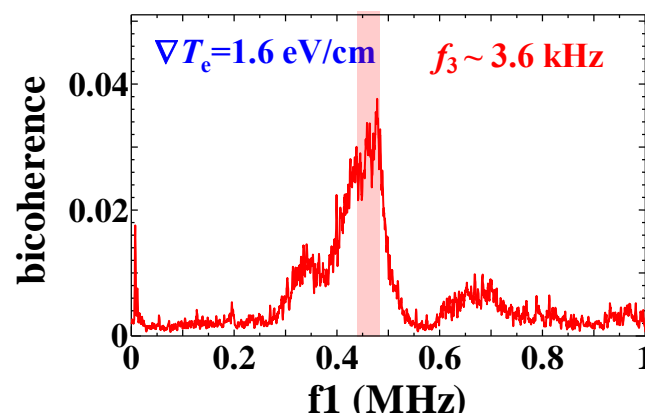
# Bicoherence of the High & Low Frequency Fluctuations

19

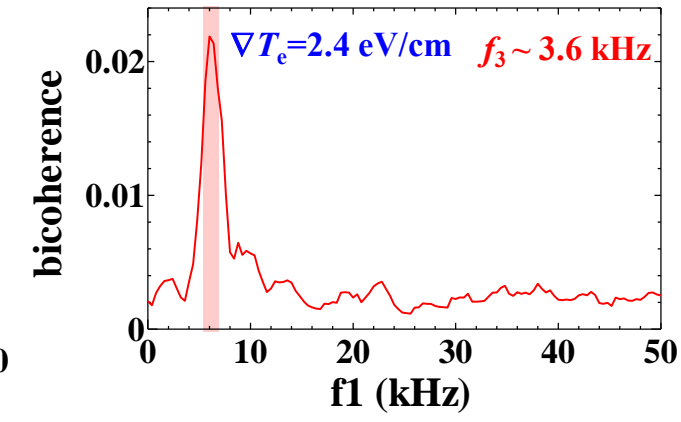
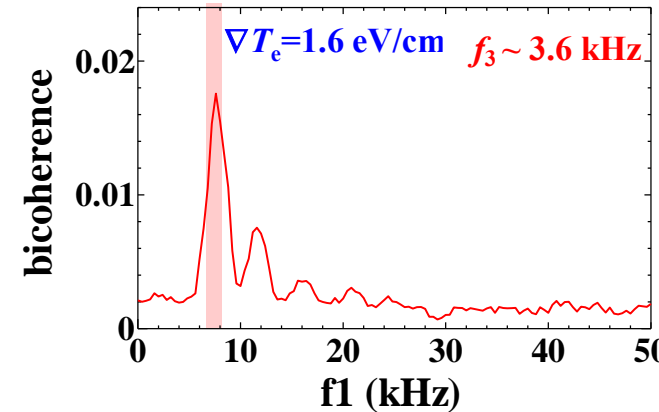
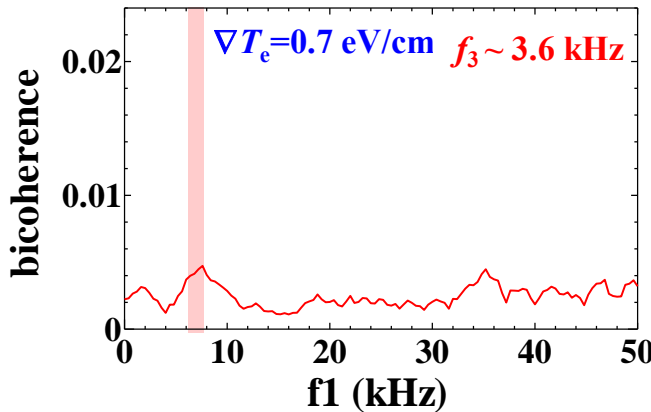
**ETG mode ( $f_2 = \sim 0.4$  MHz)**



$P_\mu = 20 \text{ W}$ ,  $V_{g1} = -10 \text{ V}$ ,  $V_{ee1} = -4.0 \text{ V}$ ,  
 $V_{ee2} = -1.5 \text{ V}$ ,  $r = -0.9 \text{ cm}$



**DW mode ( $f_2 = \sim 7$  kHz)**

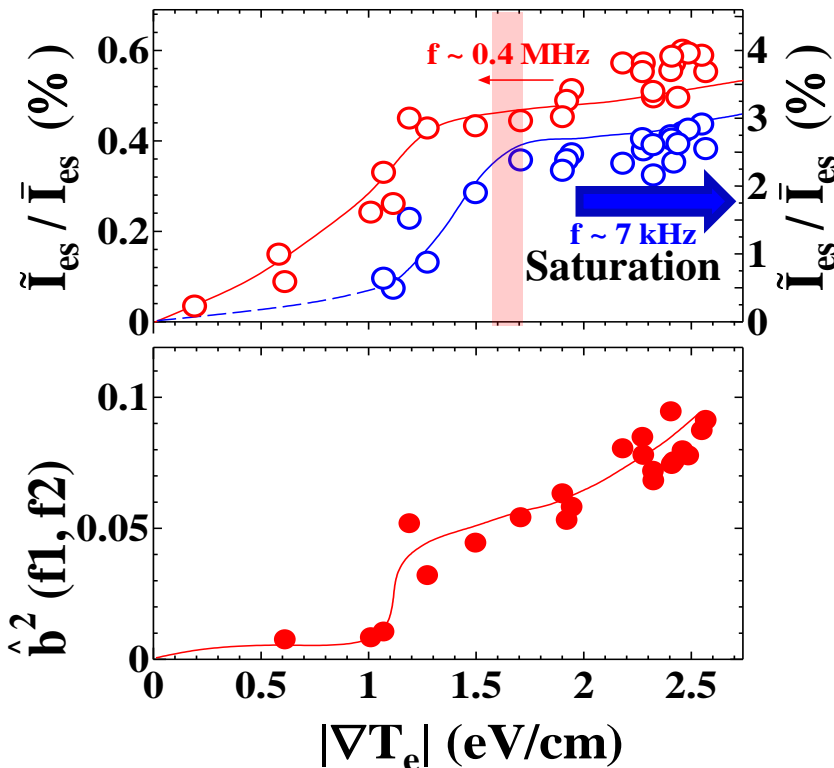


The slice of bicoherence between the DW mode and the flute mode has a noticeable peak when the magnitude of ETG is increased.

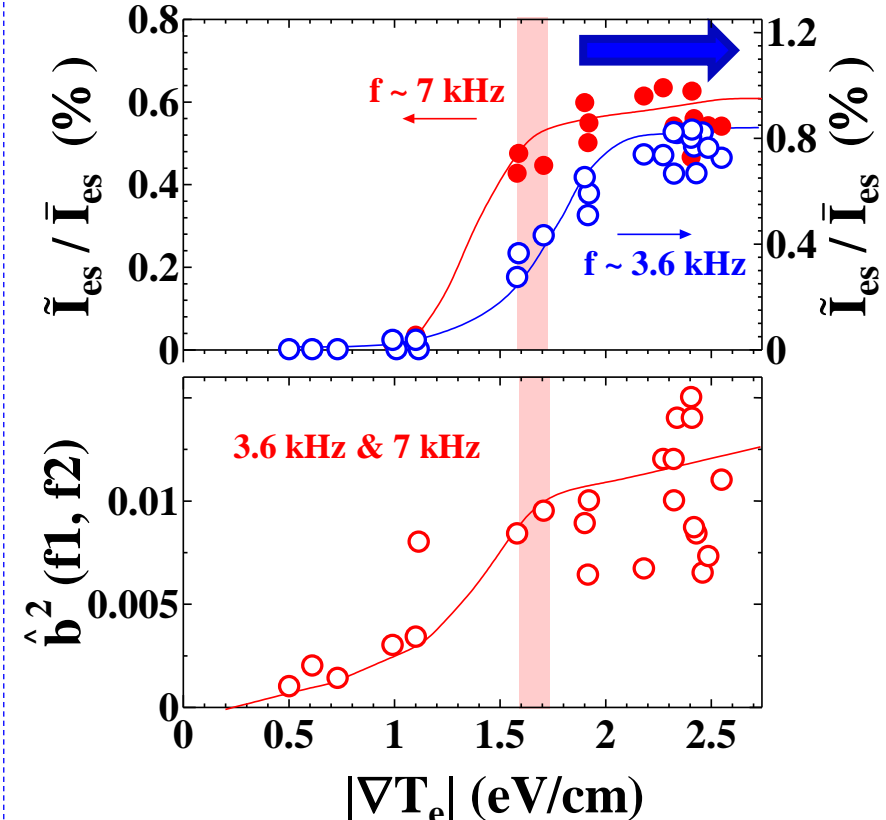
# Nonlinear Energy Transfer (flute mode)

$$P_{\mu} = 20 \text{ W}, V_{g1} = -10 \text{ V}, V_{ee1} = -4 \text{ V}, V_{ee2} = -1.5 \text{ V}, r = -0.9 \text{ cm}$$

Nonlinear interaction between  
ETG mode and DW mode



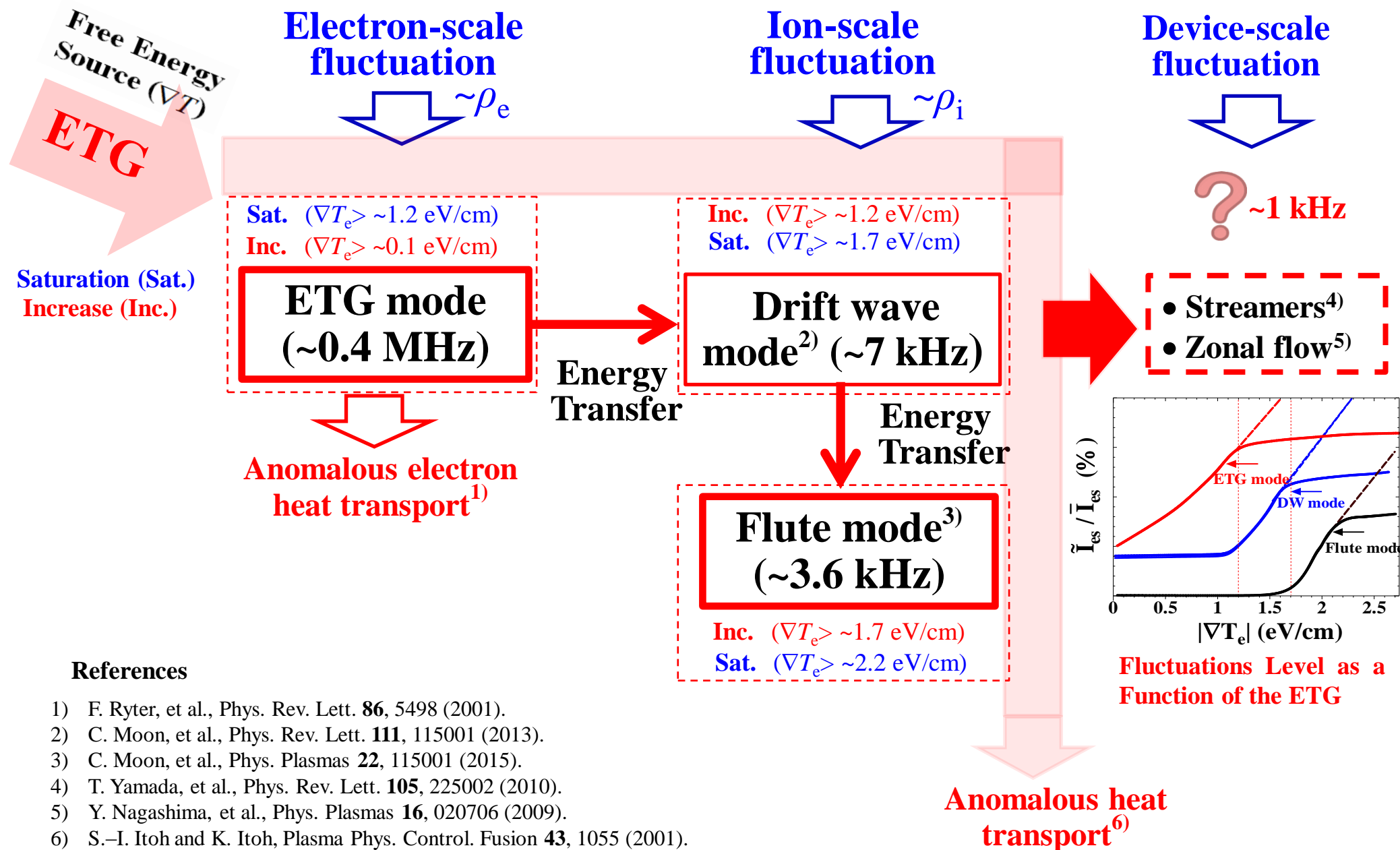
Saturation



C. Moon, et al., Phys. Plasmas 22, 052301 (2013).

It is considered that the energy of the DW mode is transferred to the flute mode through the nonlinear interaction.

# Effect of ETG on the Nonlinear Interplay



# Summary

In order to understand the electron temperature gradient (ETG) mode driven anomalous heat transport, we investigate a multi-scale nonlinear coupling between the electron-scale ETG mode and the ion-scale fluctuations in linear magnetized plasmas.

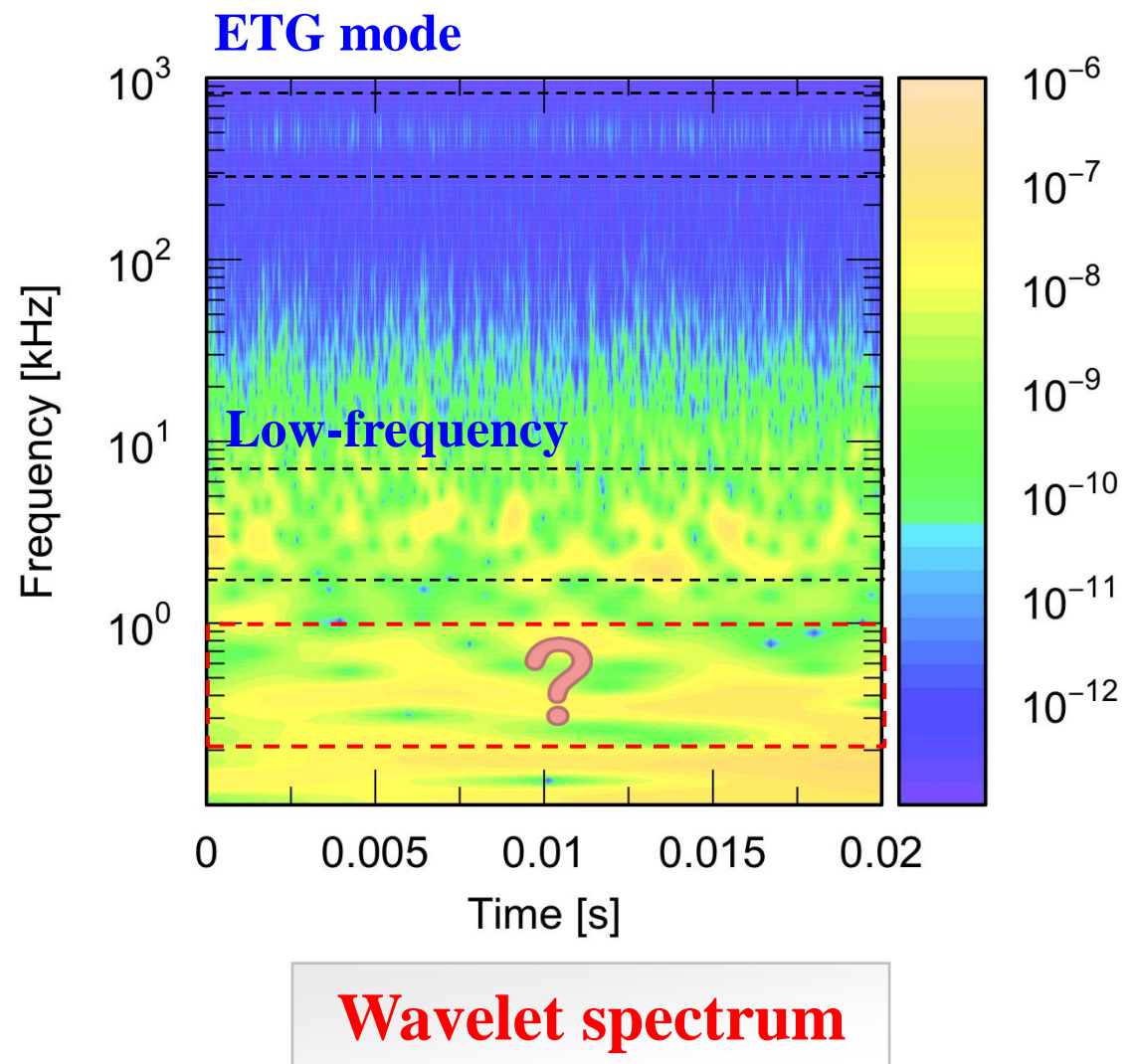
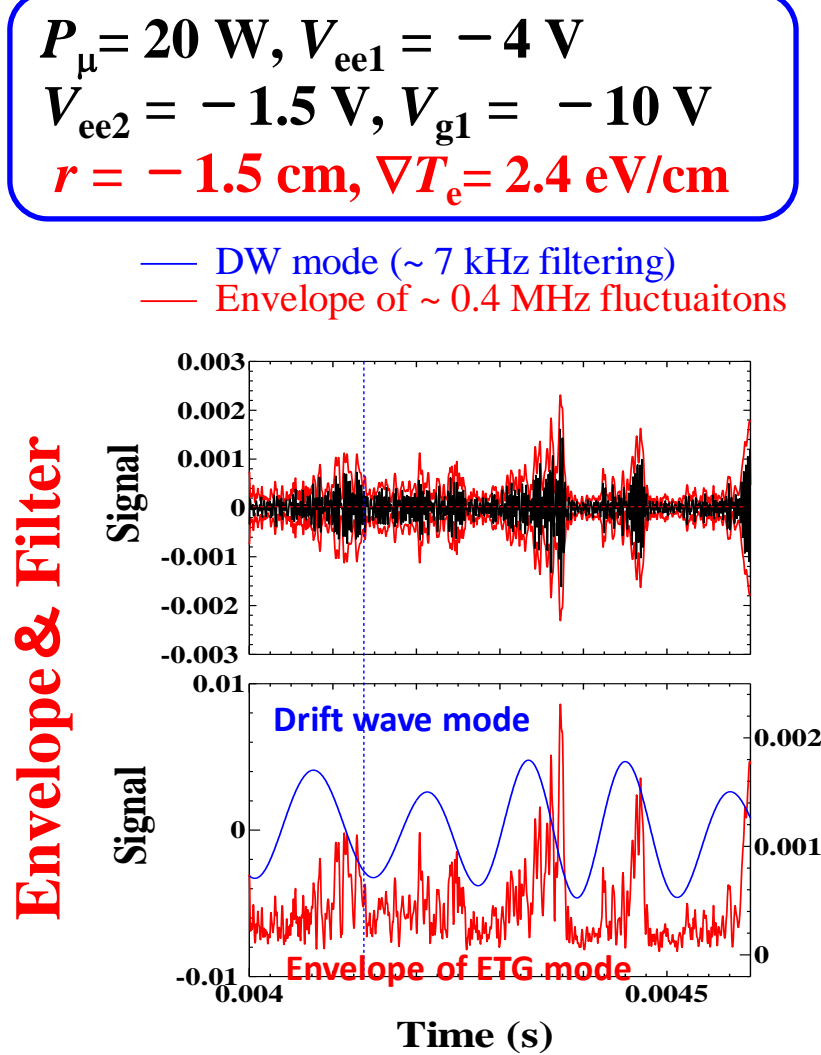
- The formed ETG is found to excite a high-frequency fluctuation ( $\sim 0.4$  MHz), i.e., ETG mode, furthermore, the drift wave (DW) mode ( $\sim 7$  kHz), which is enhanced by the nonlinear coupling with the ETG mode.
- It is observed another low-frequency ( $\sim 3.6$  kHz) fluctuation associated with the flute mode is enhanced by the nonlinear coupling with the DW mode.
- The ETG mode energy was transferred to the DW mode, and then the energy was ultimately transferred to the flute mode, which was triggered by the disparate scale nonlinear interactions between the ETG and ion-scale low-frequency modes.



## Acknowledgements

The authors acknowledge helpful discussions by Prof. S. Inagaki and Prof. S.-I. Itoh. This work was supported by the Grant-in-Aid for JSPS Fellows (23-1638), and a Grant-in-Aid for Scientific Research from the Ministry of Education, Culture, Sports, Science and Technology, Japan. This work was partly supported by the Grant-in-Aid for Scientific Research of JSPF, Japan (Nos. 15H02155 and 23244113), by the collaboration programs of the RIAM of Kyushu University and of NIFS (NIFS13KOCT001), and by the Asada Science Foundation.

# The Temporal Evolution of Fluctuations



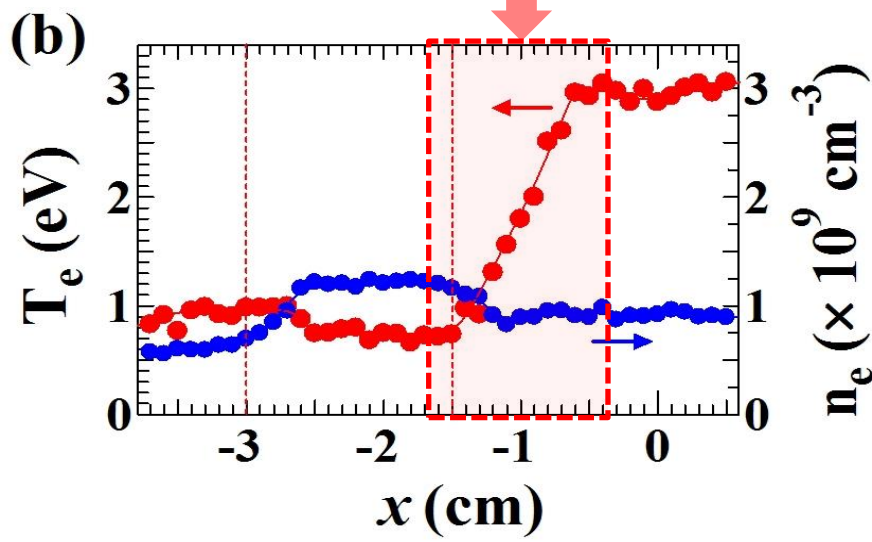
The modulation of ETG mode with low-frequency fluctuations is well observed when sufficient ETG is formed.

# プラズマの半径方向分布

25

$$P_{\mu} = 20 \text{ W}, V_{g1} = -10 \text{ V}, V_{g2} = -30 \text{ V}, \\ V_{ee1} = -4.0 \text{ V}, V_{ee2} = -1.5 \text{ V}, r = -1.5 \text{ cm}$$

PRL2013の図1

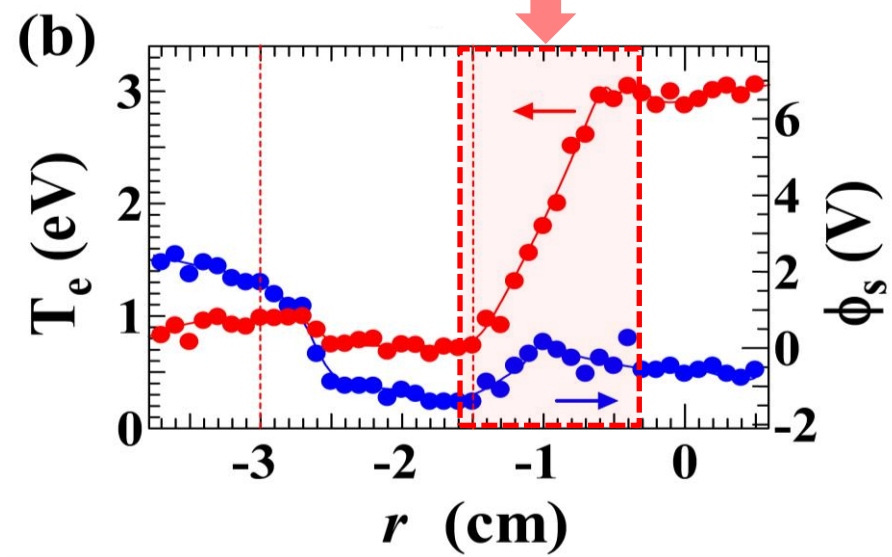


電子密度勾配が谷のように形成

A blue downward arrow points to the following equation:

$$\left| \frac{n_e^+}{n_e^-} \right| = 14.5 \text{ } m^{-1}$$

POP2015の図2



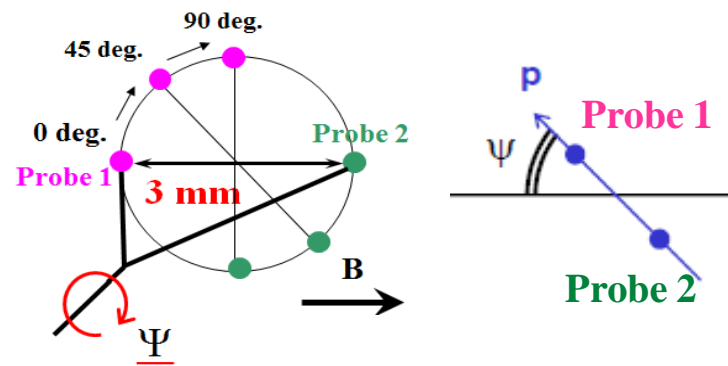
$E_r \simeq +0.1 \text{ (V/cm)}$

$E \times B$  方向はイオン反磁性方向

# 位相差測定によるモード数の同定(密度揺動のみ)

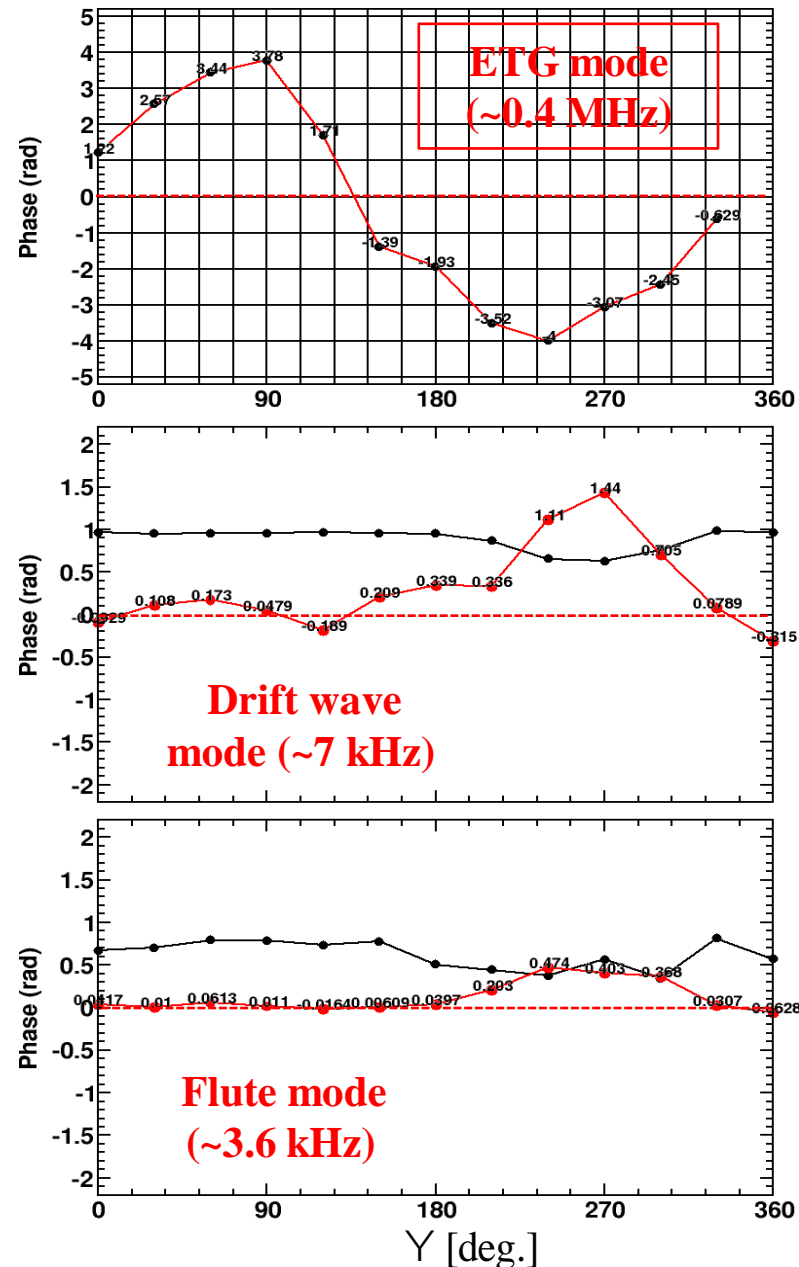
26

$$\begin{aligned}
 P_\mu &= 20 \text{ W}, \\
 V_{g1} &= -10 \text{ V}, \\
 V_{g2} &= -30 \text{ V}, \\
 V_{ee1} &= -4.0 \text{ V}, \\
 V_{ee2} &= -1.5 \text{ V}, \\
 r &= -1.5 \text{ cm}
 \end{aligned}$$

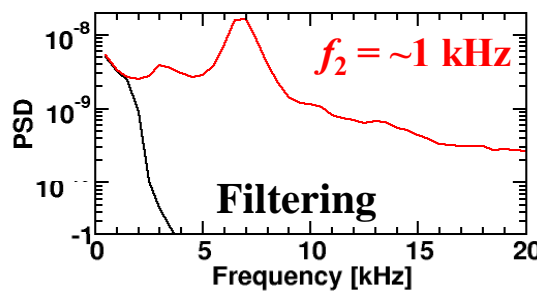
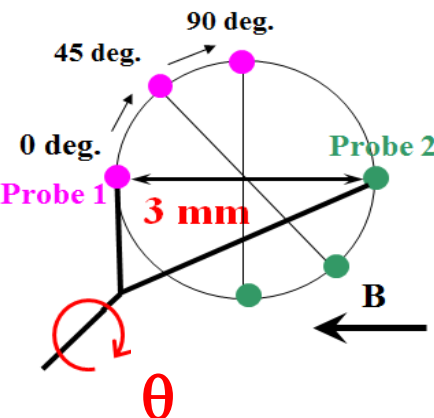
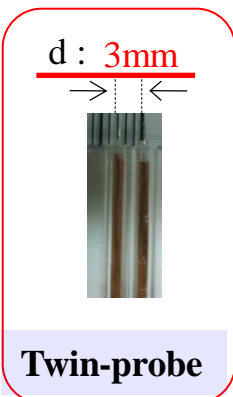


磁場に垂直( $\theta$ )方向への伝搬方向とそのモード数

	ETG	DW	flute
<i>mode number</i>	~40	~8	~2
波長 $\lambda$ (mm)	~2.4	~11.5	~44.9
周波数 $f$ (kHz)	460	7	3.6
伝搬方向	電子反磁性	イオン反磁性(?)	イオン反磁性(?)

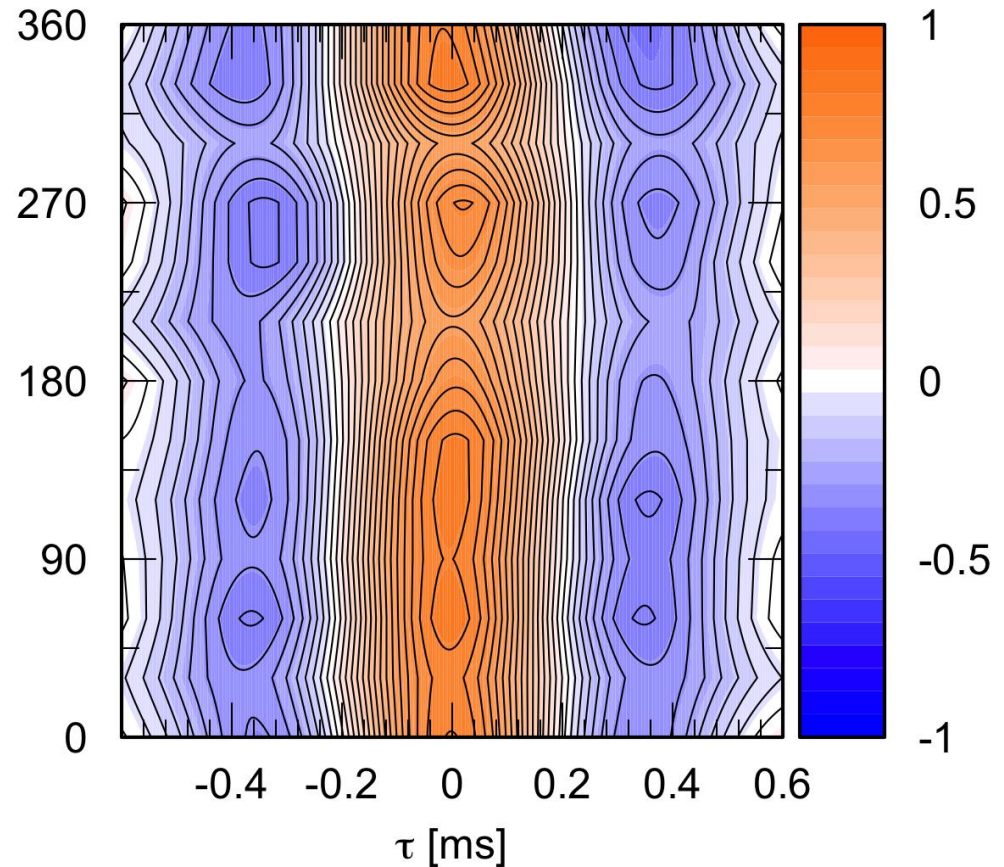


# Spatial Structure of the Lower-frequency Fluctuations 27



$P_\mu = 20\text{ W}$ ,  $V_{g1} = -10\text{ V}$ ,  $V_{ee1} = -4.0\text{ V}$ ,  $V_{ee2} = -1.5\text{ V}$ ,  
 $V_{g2} = -30\text{ V}$  ( $\nabla T_e = 2.4\text{ eV/cm}$ ).

Cross-Correction with  $\tilde{n}$  and  $n$

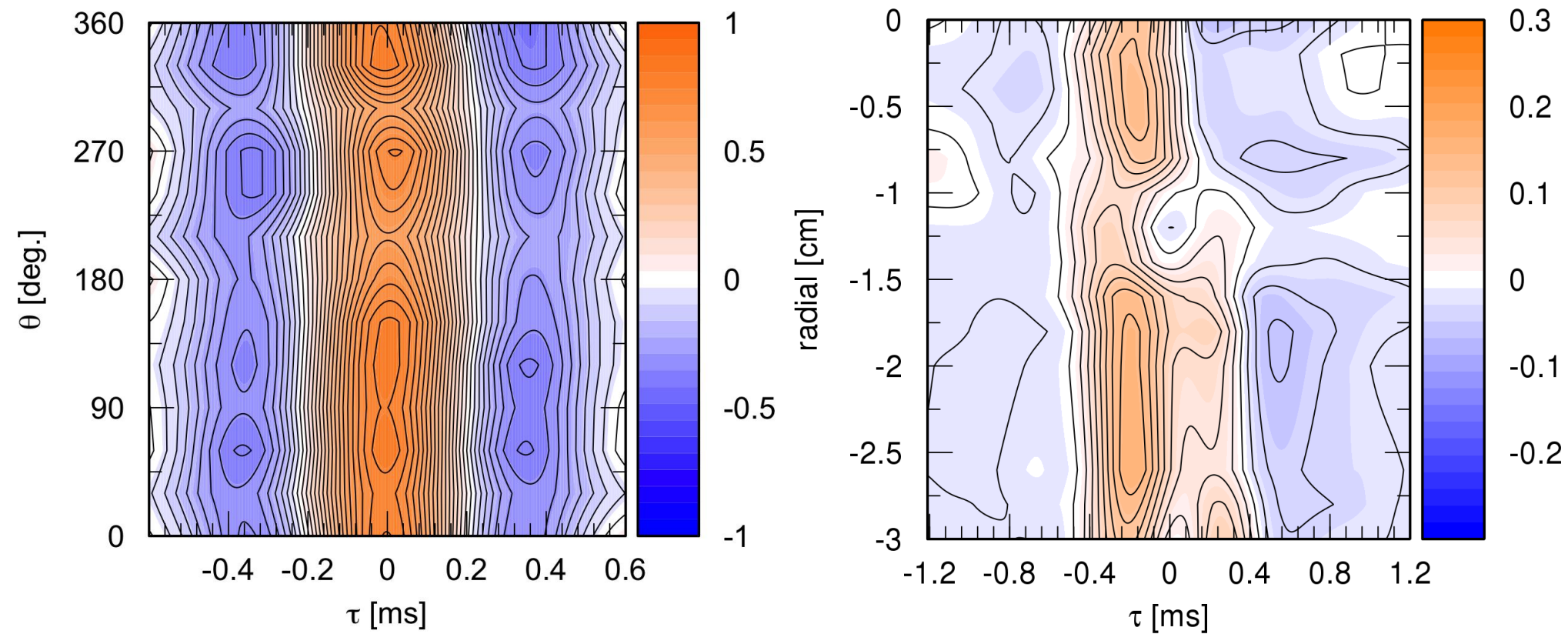


It is found that the fluctuations with  $f \simeq 1\text{ kHz}$  is the poloidal wave number  $k_\theta = 0$  ( $m \sim 0$ ).

# Spatial Structure of Low-frequency Fluctuations

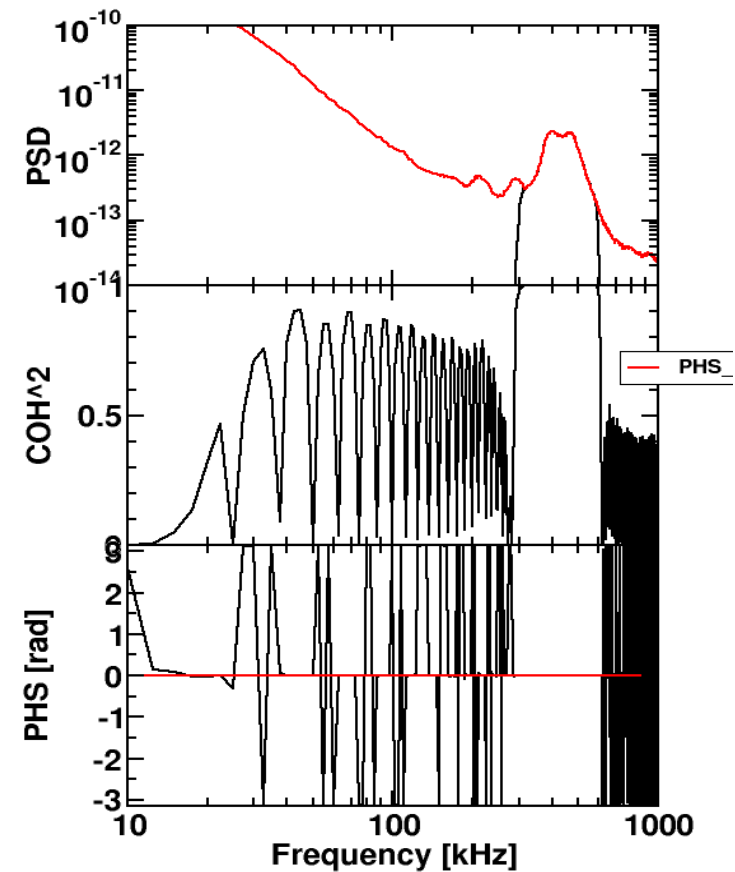
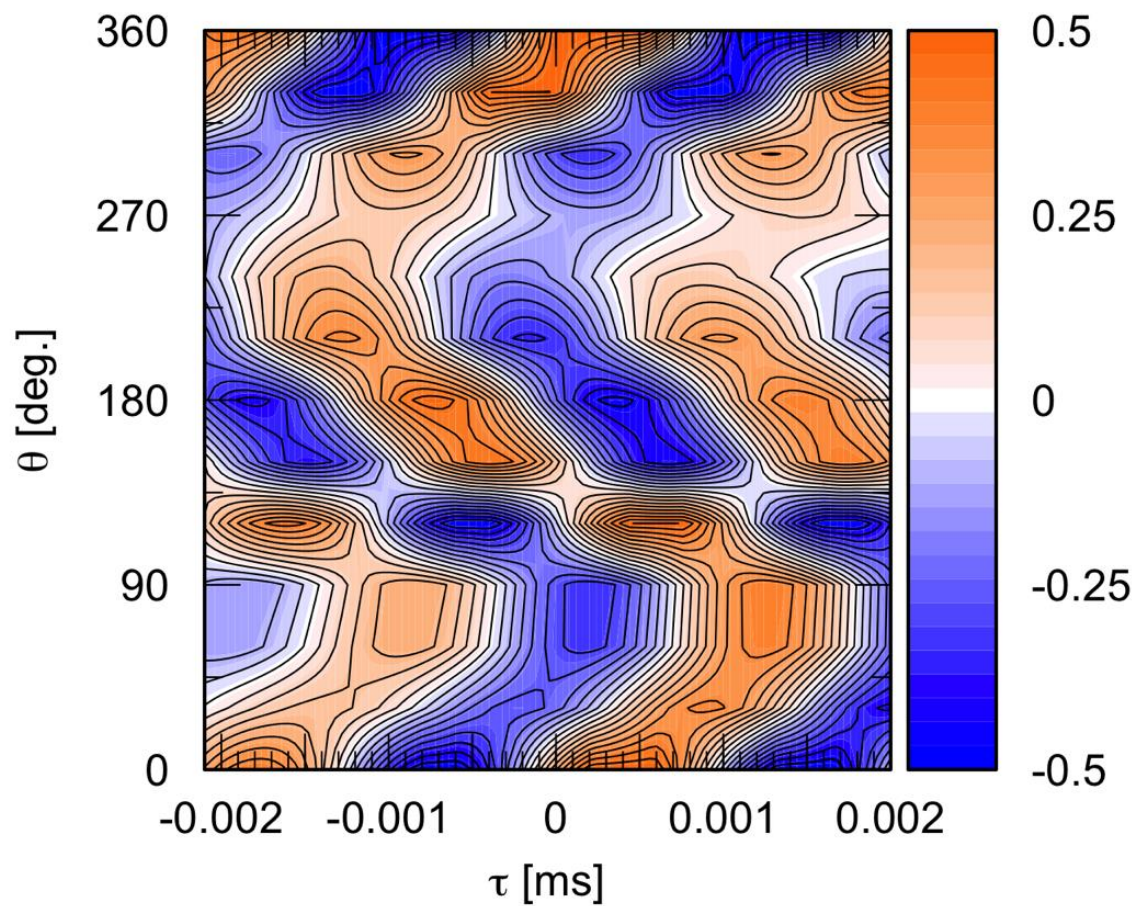
28

Cross-Correction with  $\tilde{n}$  and  $\tilde{n}$



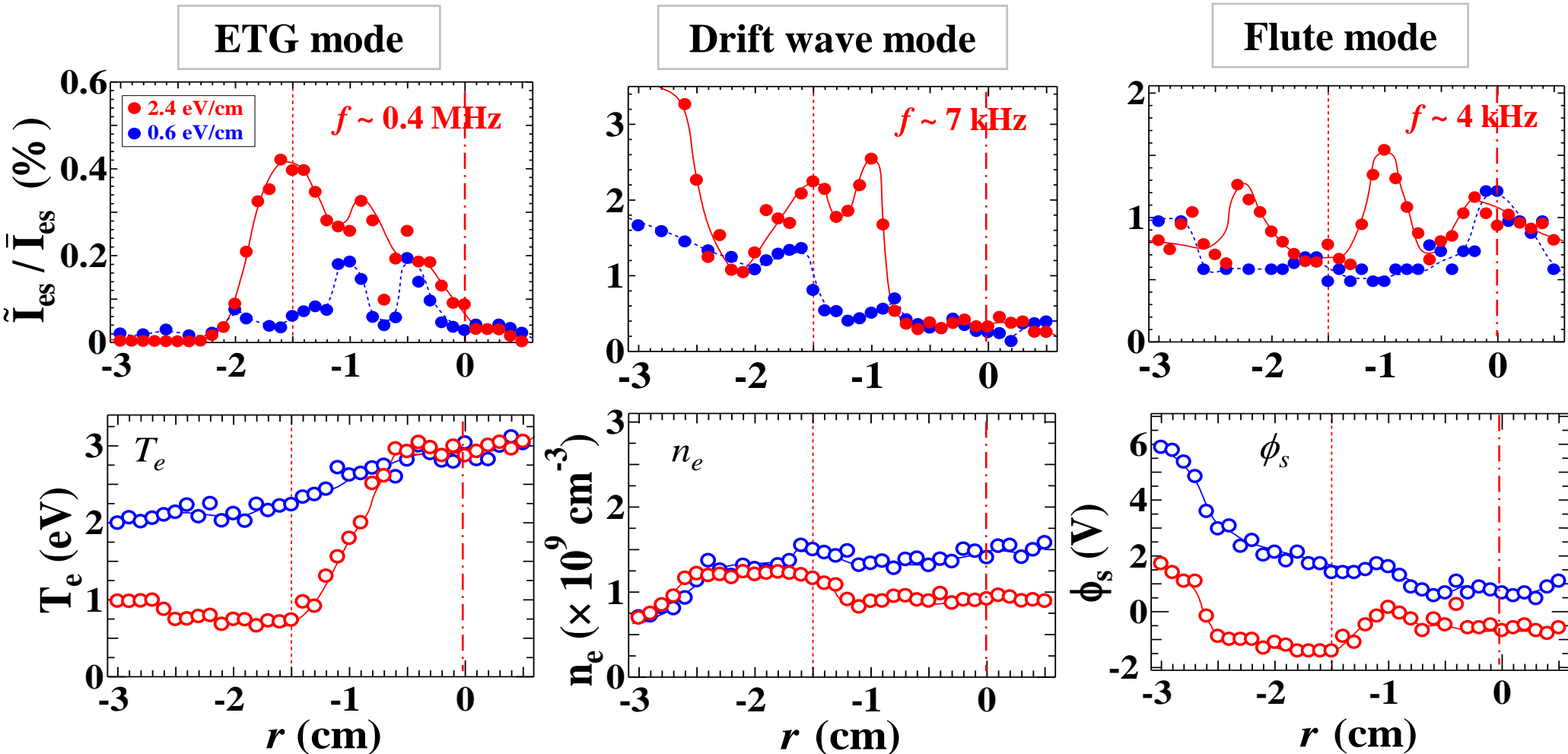
# Spatial Structure of ETG mode

29



# Radial Profiles of ETG driven Fluctuations

$P_\mu = 20 \text{ W}$ ,  $V_{g1} = -10 \text{ V}$ ,  $V_{g2} = -30 \text{ or } 3 \text{ V}$ ,  $V_{ee1} = -4 \text{ V}$ ,  $V_{ee2} = -1.5 \text{ V}$



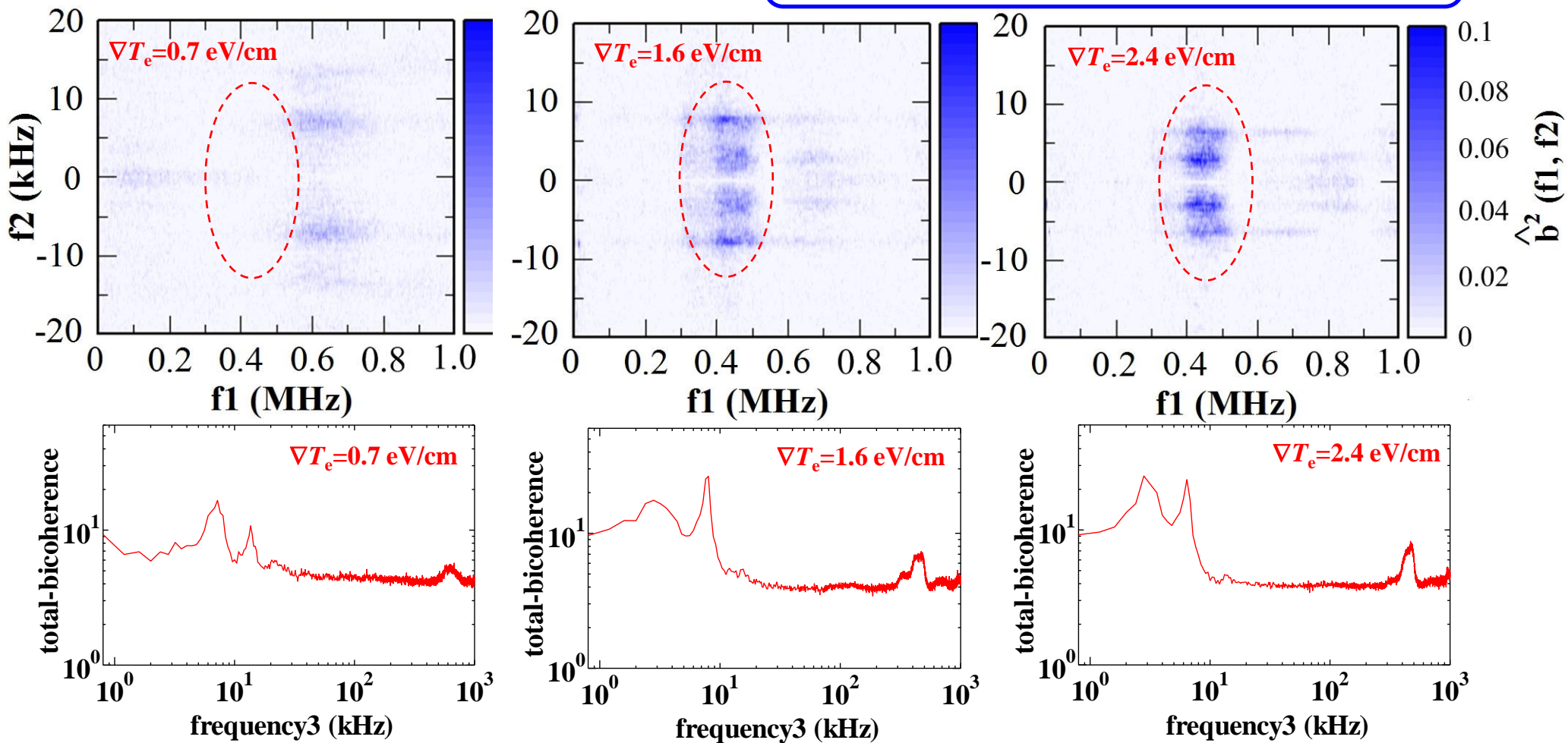
It is observed another low-frequency ( $\sim 4 \text{ kHz}$ ) mode when the electron temperature gradient  $\nabla T_e$  exceeds a certain threshold.

# Bicoherence of the High & Low Frequency Fluctuations

31

## Squared Bicoherence

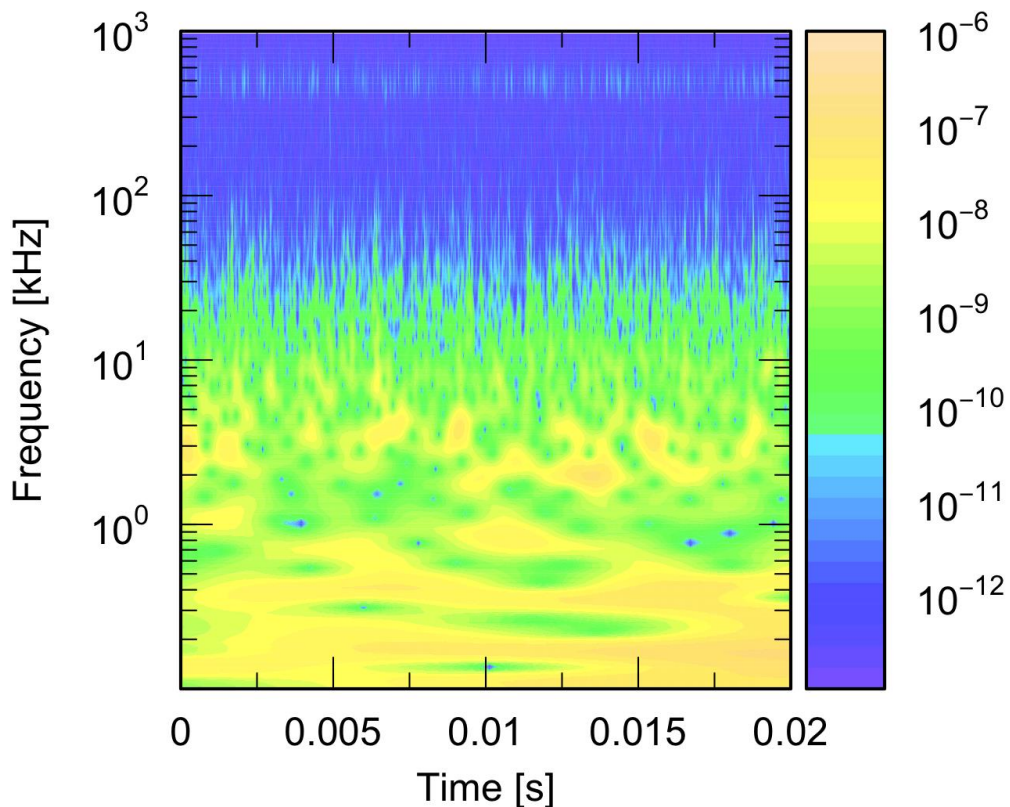
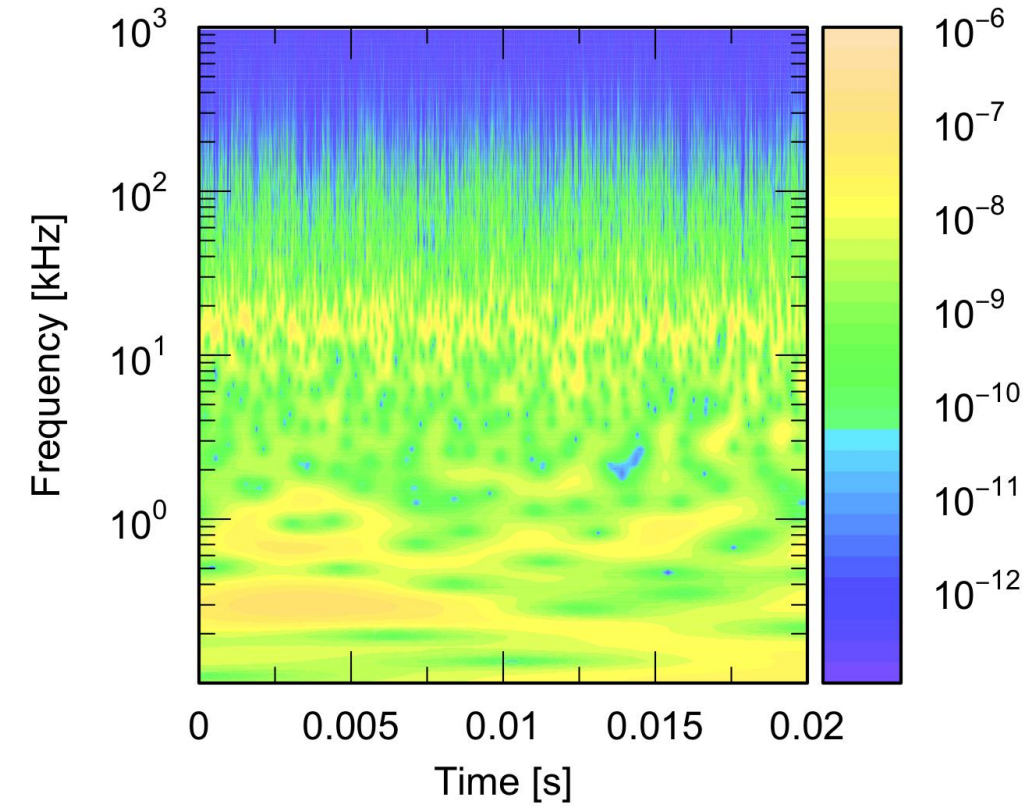
$$P_{\mu} = 20 \text{ W}, V_{g1} = -10 \text{ V}, V_{ee1} = -4.0 \text{ V}, \\ V_{ee2} = -1.5 \text{ V}, r = -0.9 \text{ cm}$$



The nonlinear couplings between the ETG mode and the ion-scale Fluctuations become stronger as the magnitude of ETG is increased.

# The Temporal Evolution of Fluctuations

$$P_{\mu} = 20 \text{ W}, V_{ee1} = -4 \text{ V}, V_{ee2} = -1.5 \text{ V}, V_{g1} = -10 \text{ V}, r = -1.5 \text{ cm}$$



The modulation of ETG mode with low-frequency fluctuations is well observed when sufficient ETG is formed.

# 付録 1: ETG モードの機構

33

- 圧力勾配による力  $F$

$$F = -\nabla p_{e,i} / n_0 = -kT_{e,i} \nabla n_0 / n_0$$

$$p = nkT$$

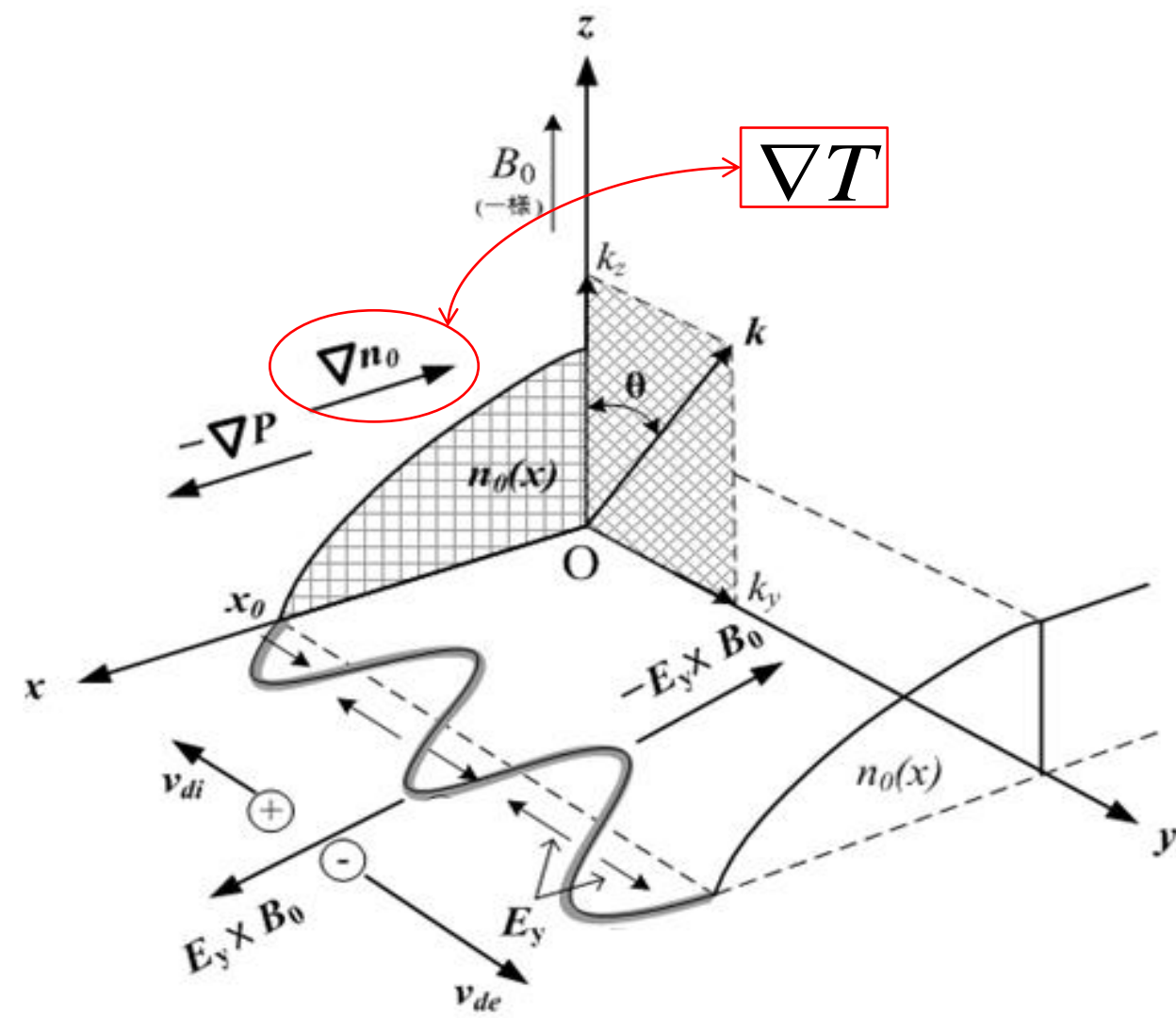
ドリフト不安定性場合

$$\nabla p = T k \nabla n$$

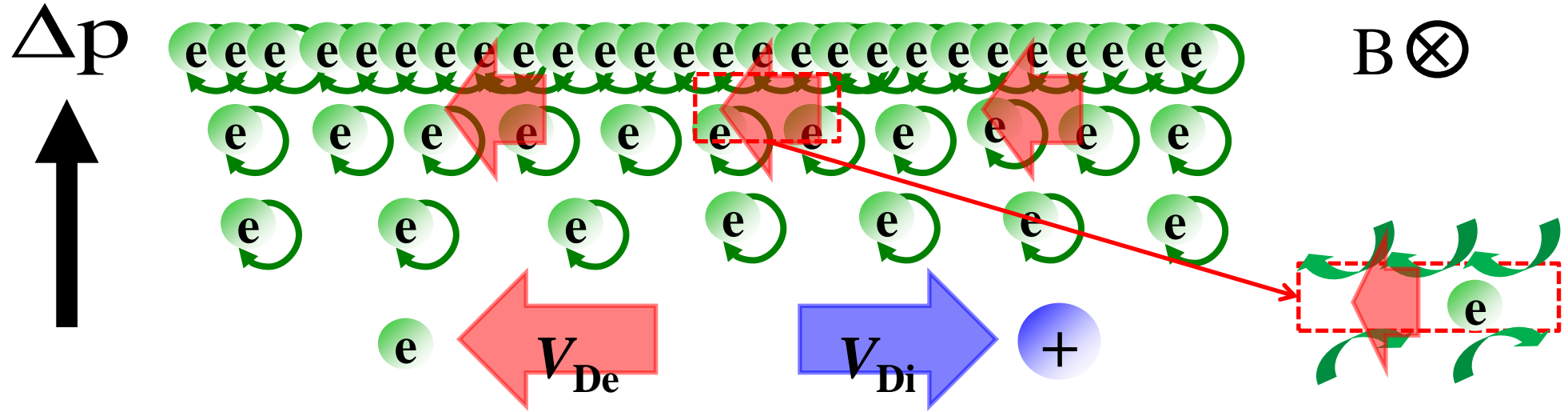
- ① わずかの波状の外乱.
- ② 正負電荷のドリフト運動が発生.
- ③ 荷電分離が生じて電界  $E$  が誘起.
- ④  $E \times B$  ドリフトによって  $x$  の正負両方向に波状の変位が助長される.

ETG 不安定性場合

$$\nabla p = nk \nabla T$$



## 付録 2: 反磁性ドリフト



プラズマの圧力によって各粒子が受ける力は

$$\mathbf{F} = -\frac{1}{n} \nabla p$$

これは(仮想的な)反磁性ドリフトである。  
これはイオンと電子に対してドリフトの  
方向が異なるため電流を生ずる。

$$V_{de} = -\frac{\mathbf{B} \times \nabla p}{enB^2} = \frac{k_b T_e}{eB} \frac{n'}{n} = \frac{k_b T_e}{eB} \frac{T'_e}{T_e}$$

$$V_{di} = -\frac{\mathbf{B} \times \nabla p}{enB^2} = \frac{k_b T_e}{eB} \frac{n'}{n} = \frac{k_b T_e}{eB} \frac{T'_e}{T_e}$$

これから反磁性電流は

$$j_D = ne(v_{Di} - v_{De}) = k_B(T_i + T_e) \frac{\mathbf{B} \times \nabla n}{B^2}$$

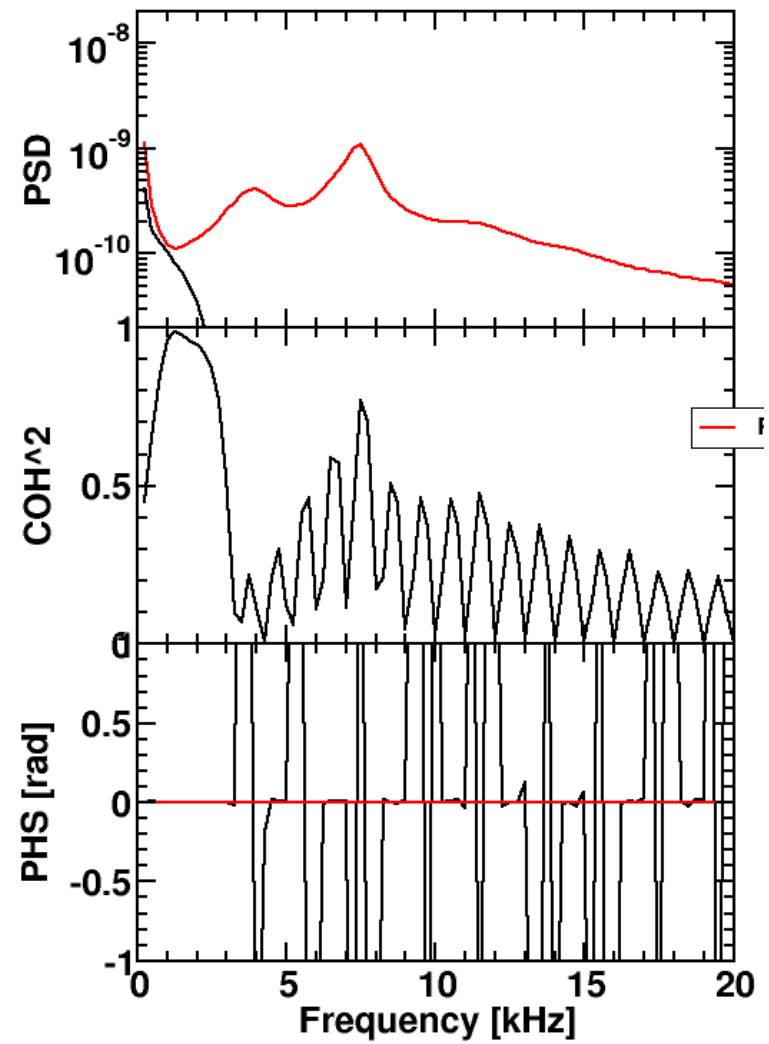
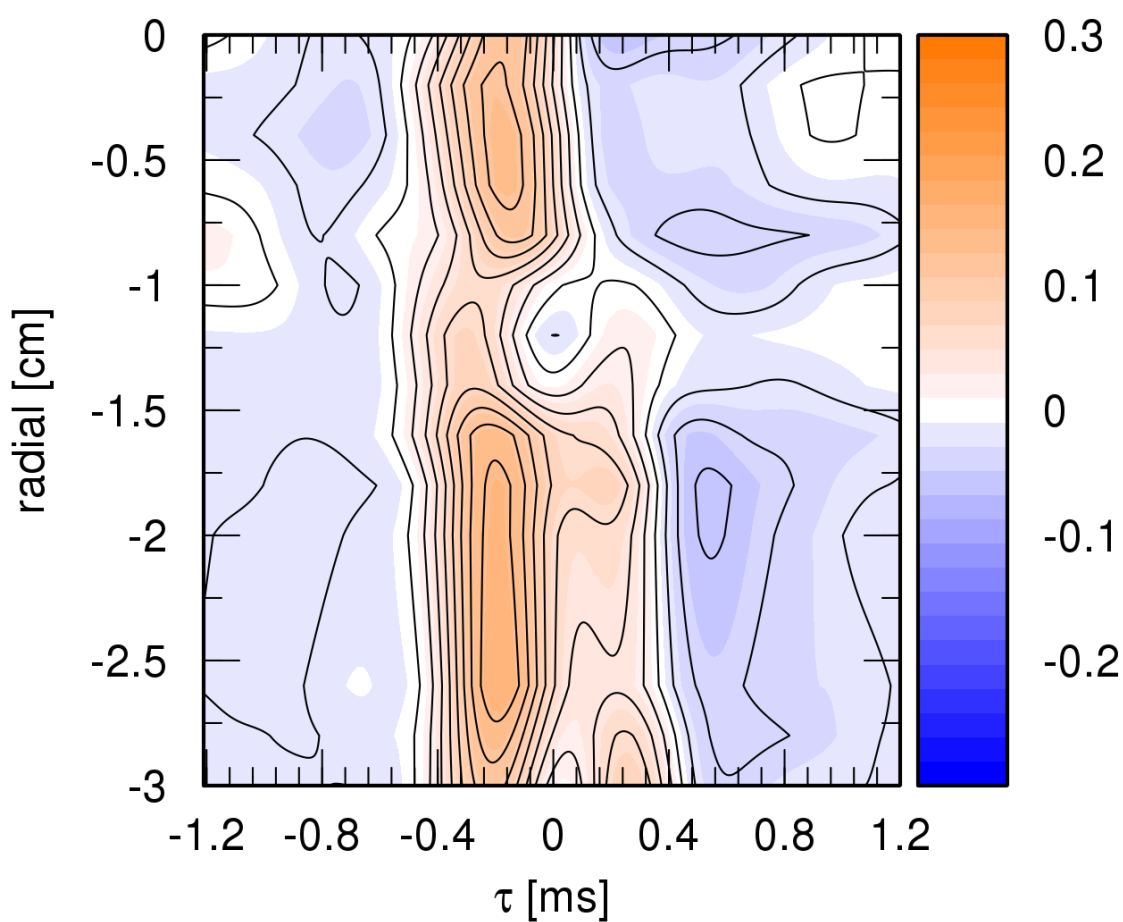
# Summary

We investigate the effects of the radial electric field ( $E_r$ ) on suppression of ETG mode through multiscale nonlinear interactions in linear magnetized plasmas.

- The formed ETG is found to excite a high-frequency fluctuation ( $\sim 0.4$  MHz), i.e., ETG mode, furthermore, the drift wave (DW) mode ( $\sim 7$  kHz), which is enhanced by the nonlinear coupling with the ETG mode.
- It is found that a sufficiently large  $E_r$  ( $E \times B$  velocity shear) can suppress the ETG mode regardless of its signs.
- The ETG mode amplitude is decreased by the energy transfer of ETG mode to DW mode through the multi-scale non-linear coupling in the slightly negative  $E_r$ .

# Nonlinear Energy Transfer

36



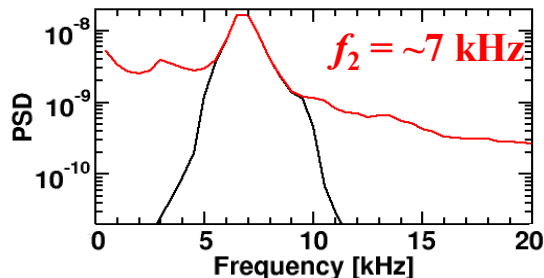
# Summary

We investigate the effects of the radial electric field ( $E_r$ ) on suppression of ETG mode through multiscale nonlinear interactions in linear magnetized plasmas.

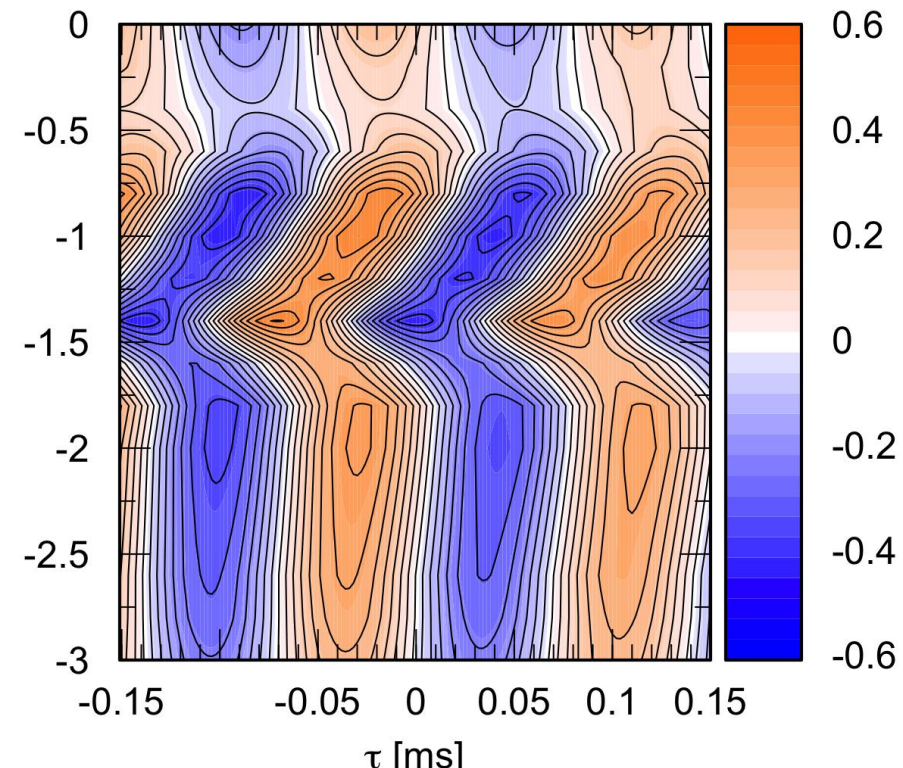
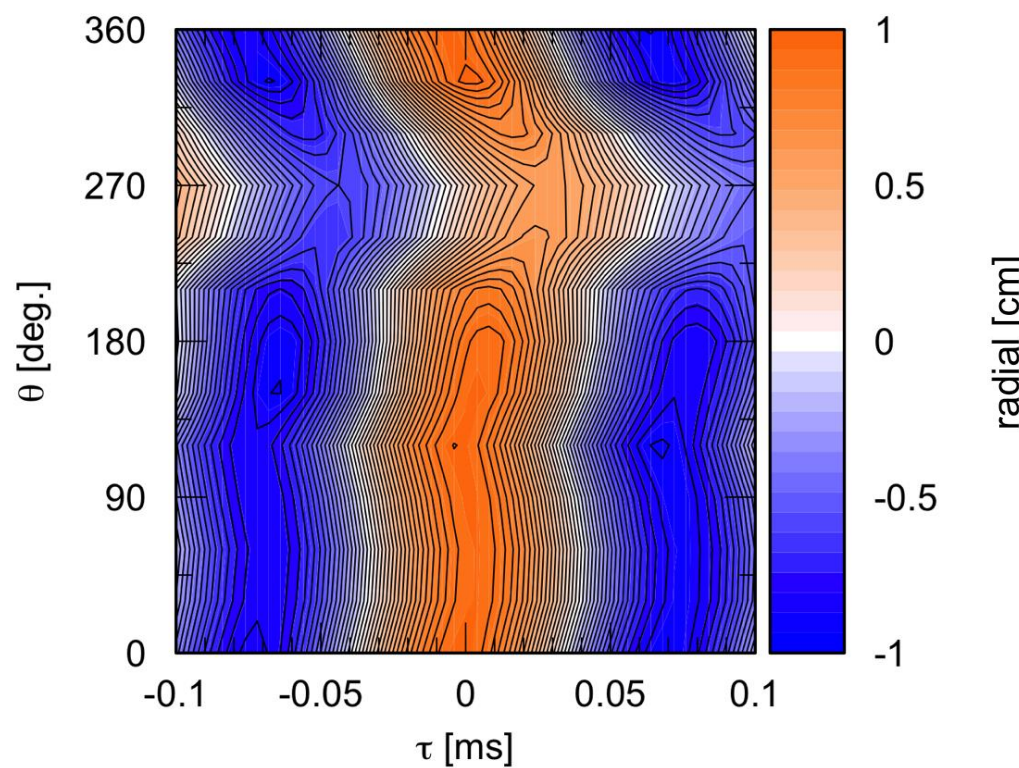
- The formed ETG is found to excite a high-frequency fluctuation (~0.4 MHz), i.e., ETG mode, furthermore, the drift wave (DW) mode (~7 kHz), which is enhanced by the nonlinear coupling with the ETG mode.
- It is found that a sufficiently large  $E_r$  ( $E \times B$  velocity shear) can suppress the ETG mode regardless of its signs.
- The ETG mode amplitude is decreased by the energy transfer of ETG mode to DW mode through the multi-scale non-linear coupling in the slightly negative  $E_r$ .

# Spatial Structure of Low-frequency Fluctuations

38



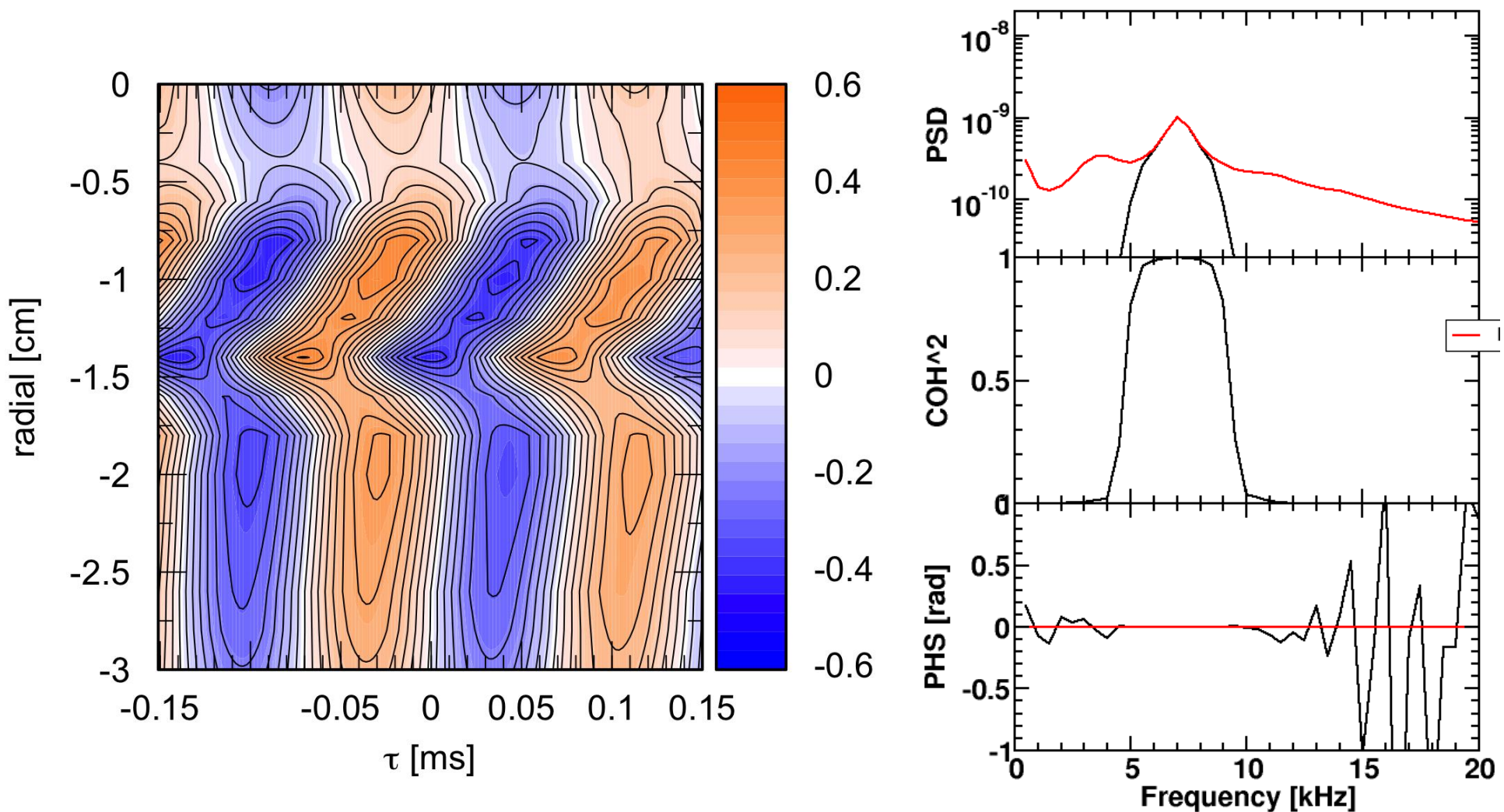
$P_\mu = 20$  W,  $V_{g1} = -10$  V,  $V_{ee1} = -4.0$  V,  $V_{ee2} = -1.5$  V,  
 $V_{g2} = -30$  V ( $\nabla T_e = 2.4$  eV/cm).



It is found that the fluctuations with  $f \simeq 7$  kHz is parallel wave number  $k_\parallel = 0$  that the energy of the DW mode is transferred to the flute mode through the nonlinear interaction.

# Nonlinear Energy Transfer

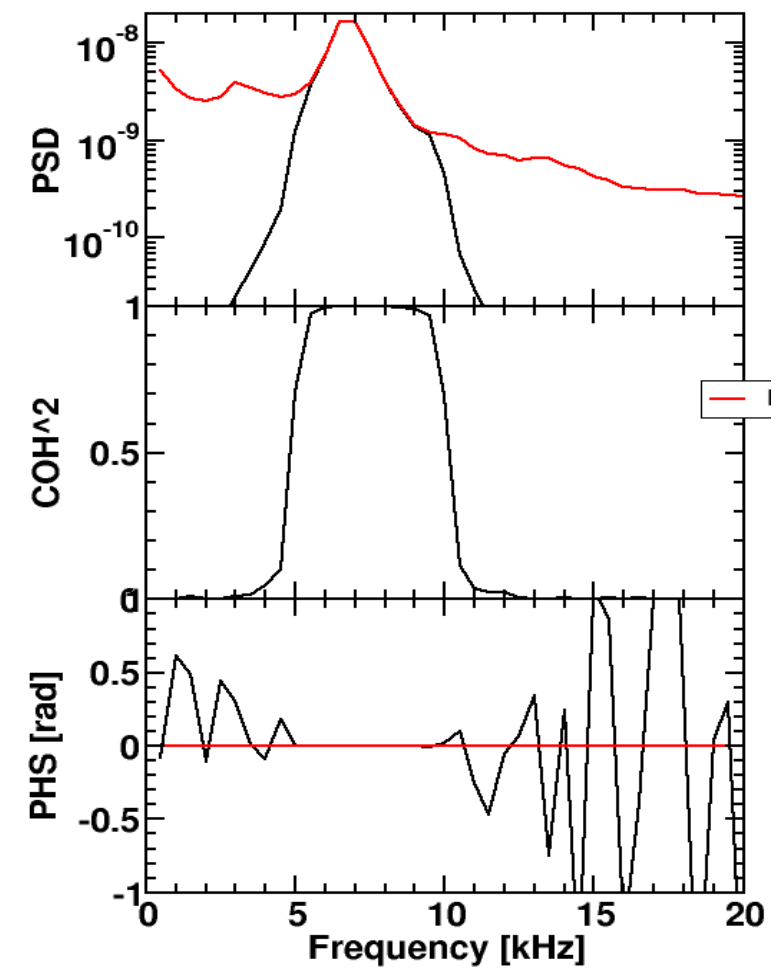
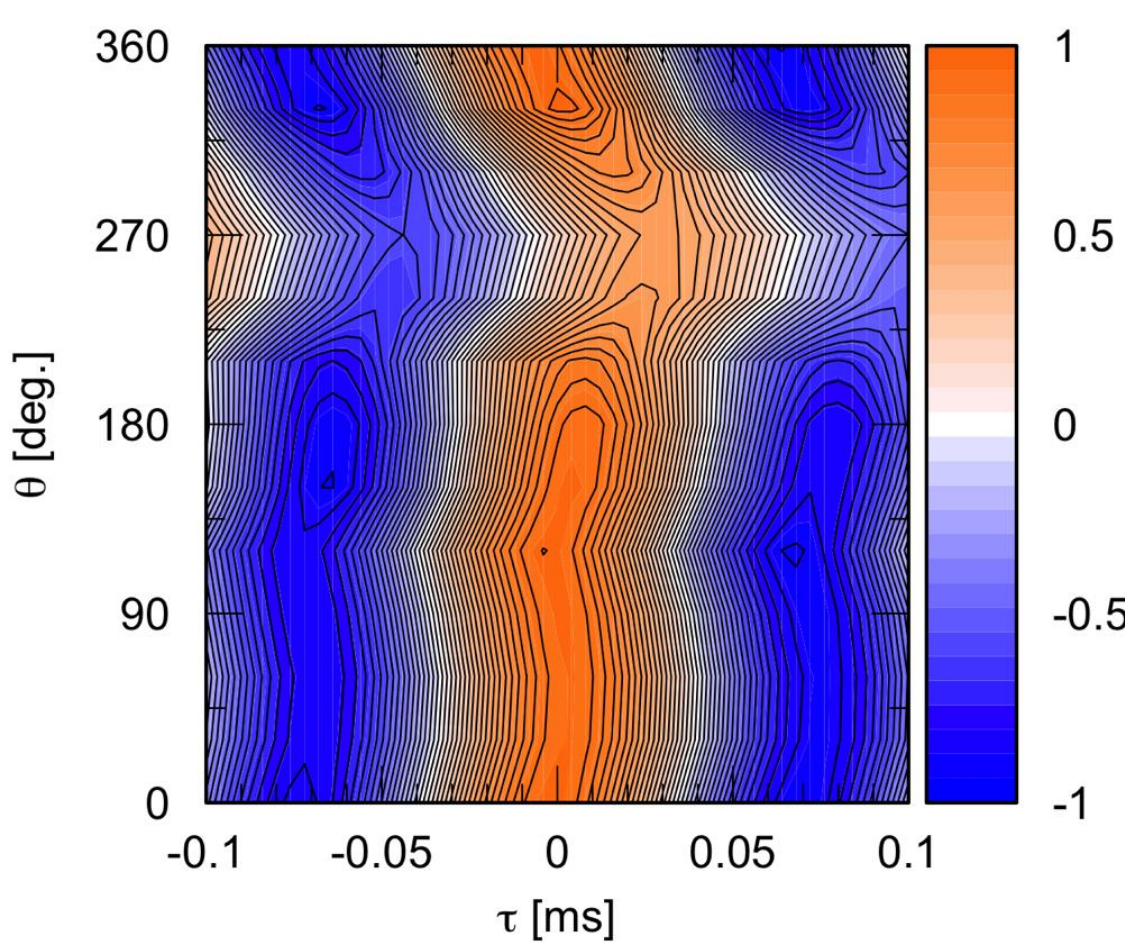
39



It is considered that the energy of the DW mode is transferred to the flute mode through the nonlinear interaction.

# Nonlinear Energy Transfer

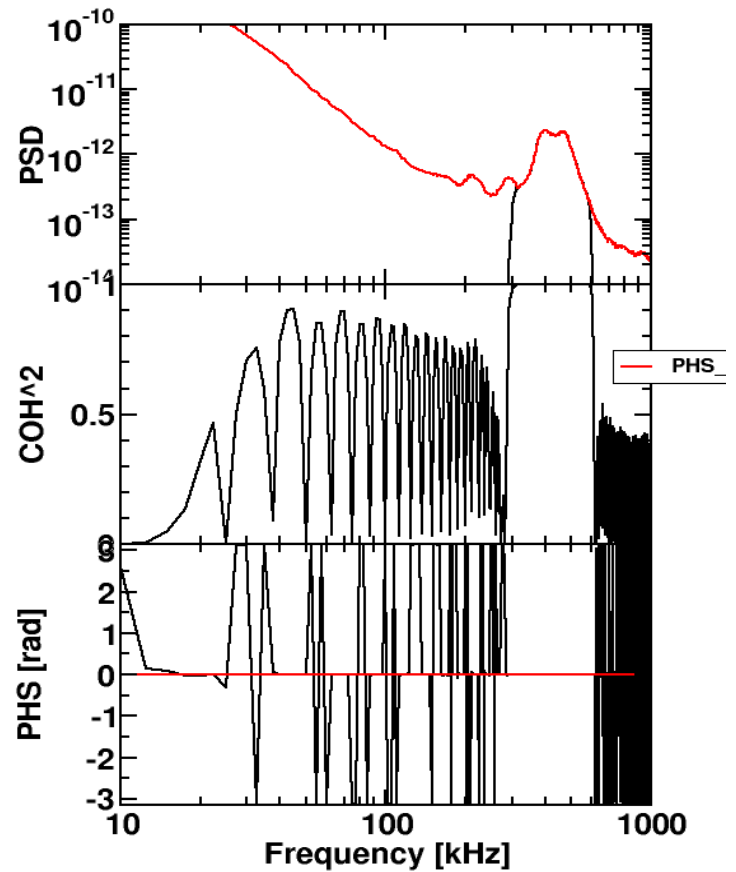
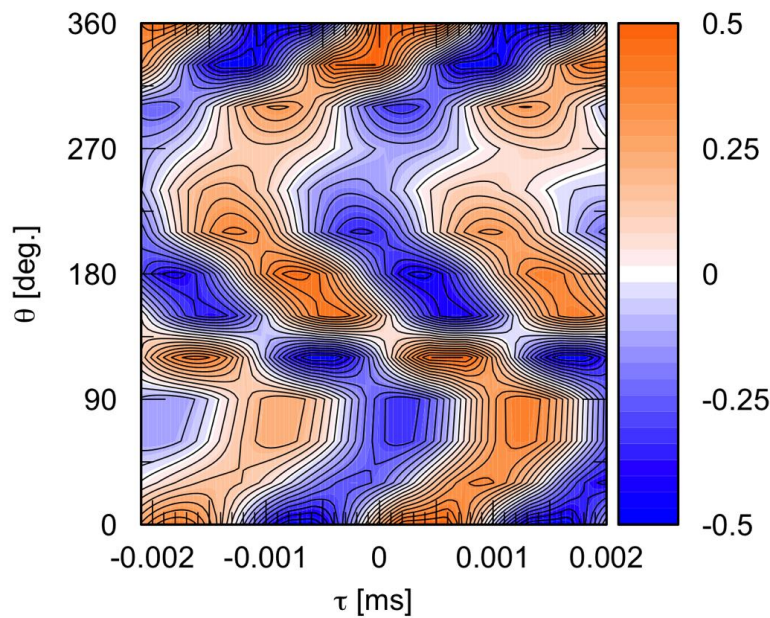
40



It is considered that the energy of the DW mode is transferred to the flute mode through the nonlinear interaction.

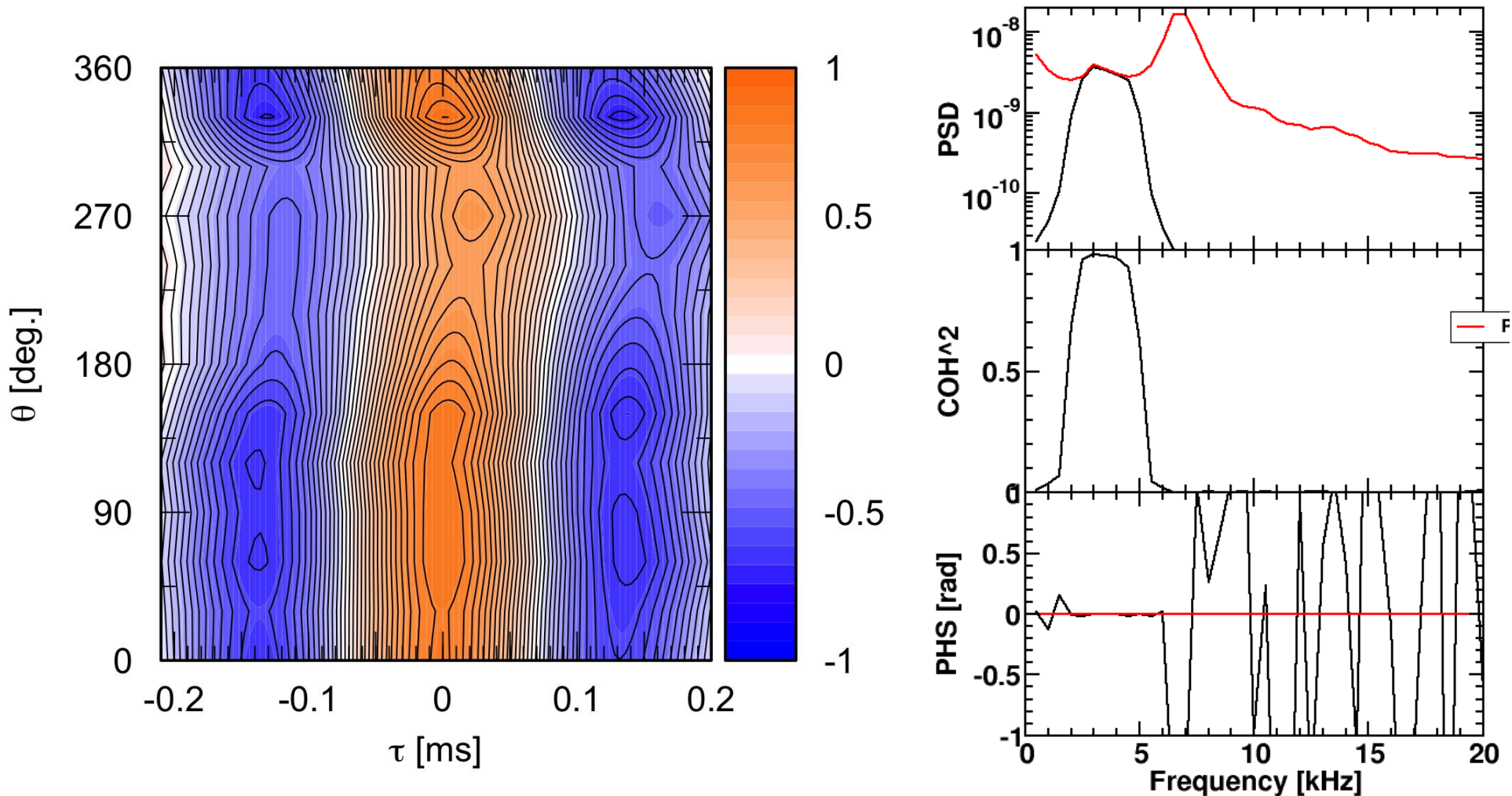
# Nonlinear Energy Transfer

41



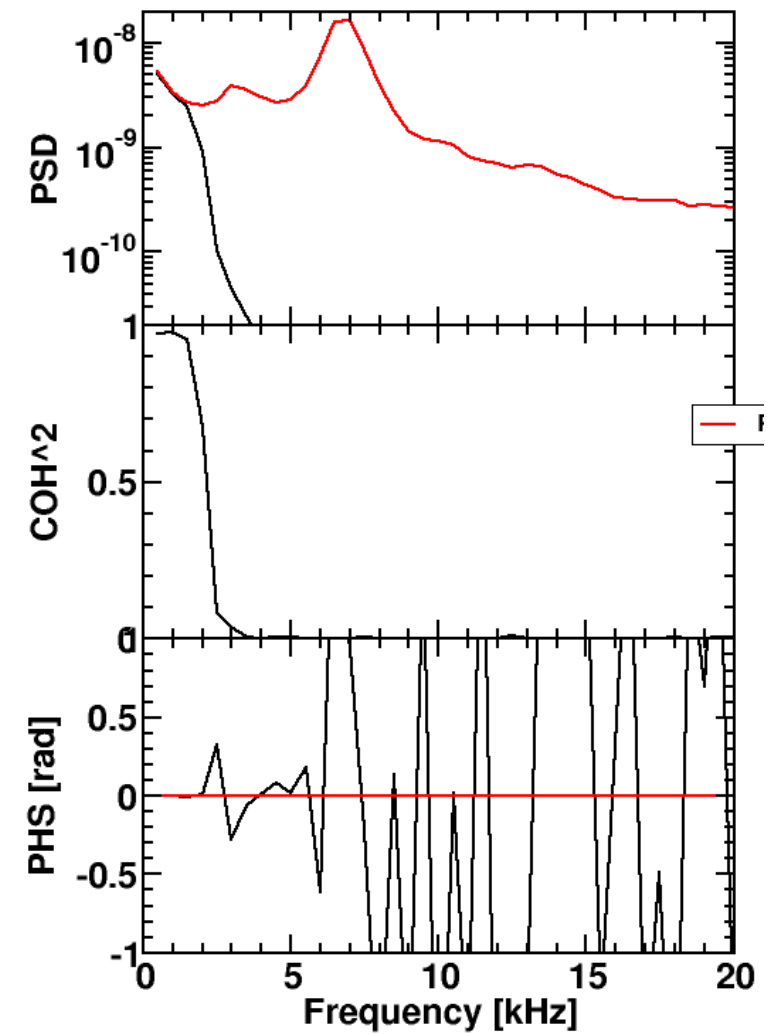
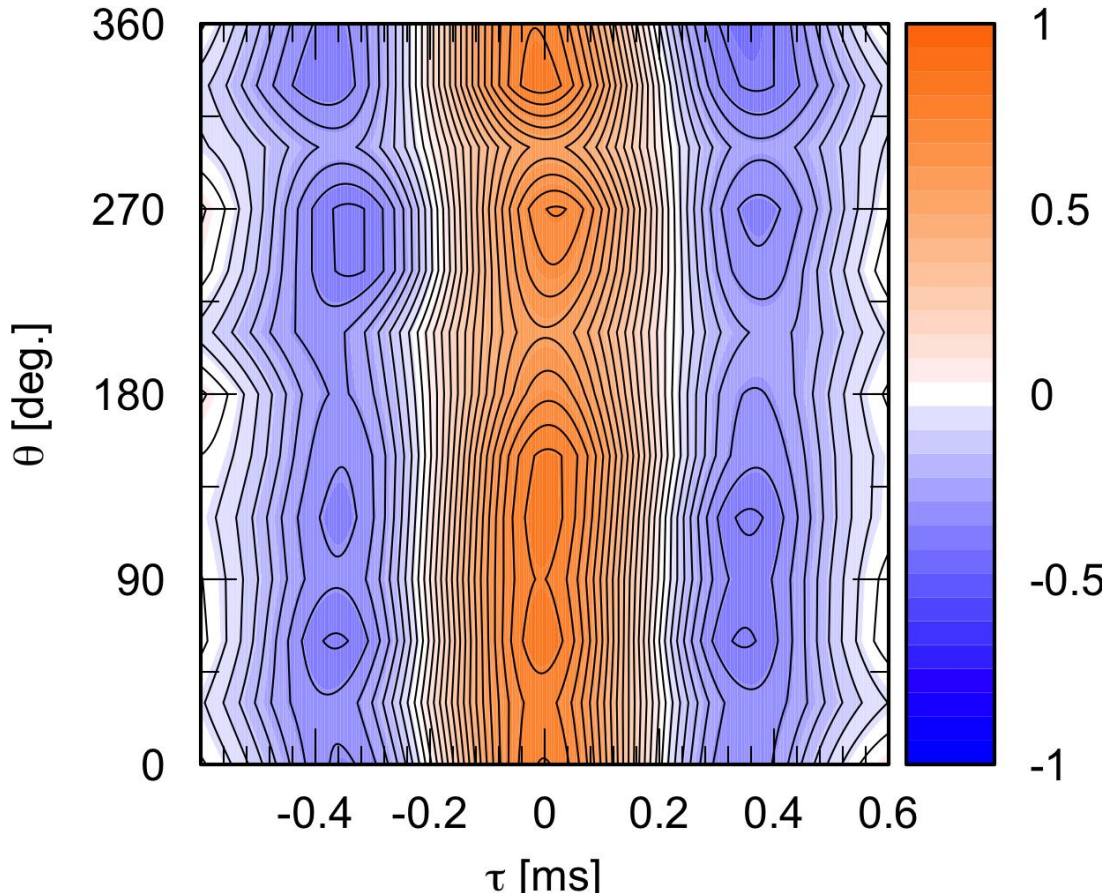
It is considered that the energy of the DW mode is transferred to the flute mode through the nonlinear interaction.

# Nonlinear Energy Transfer



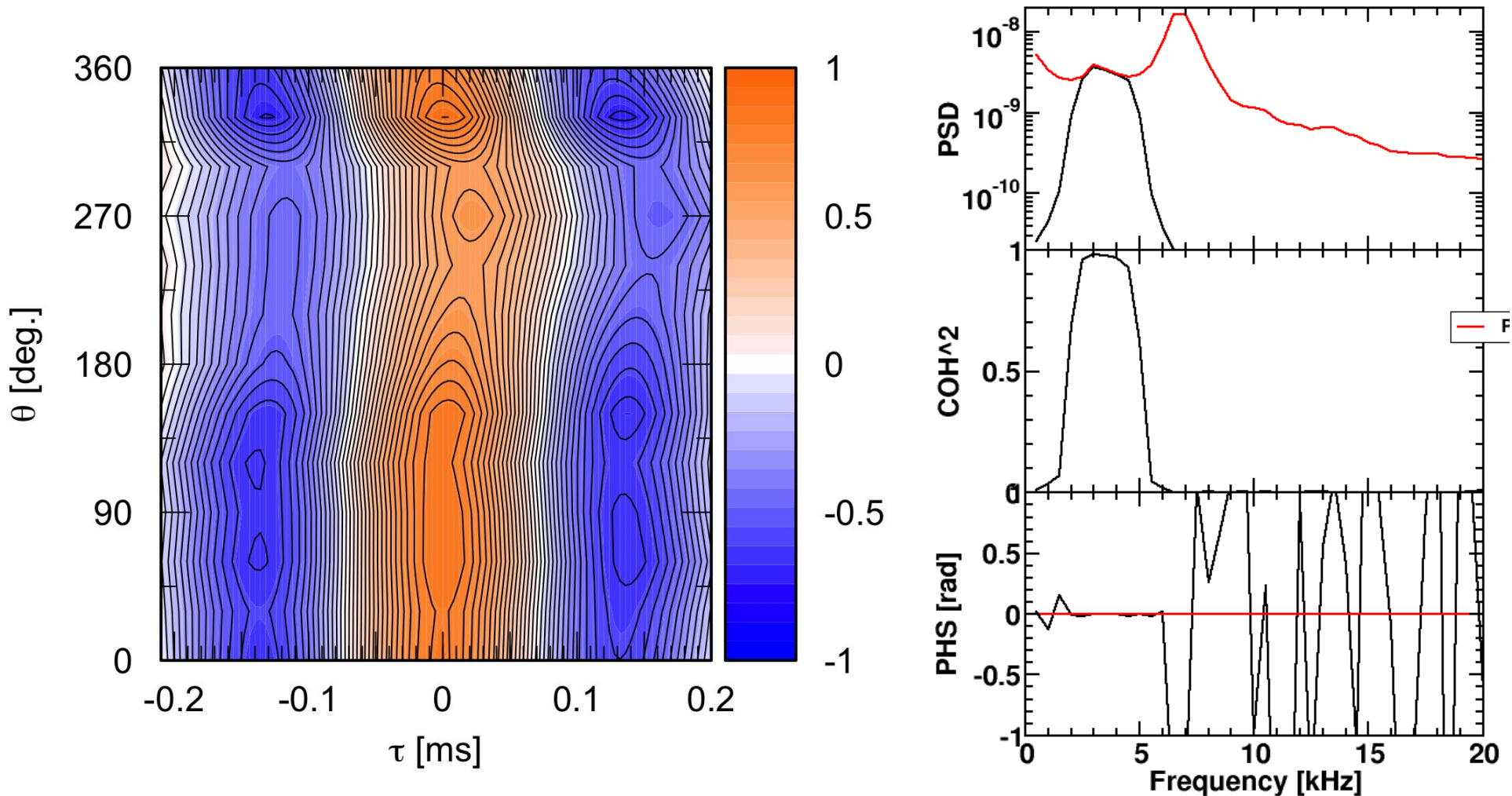
It is considered that the energy of the DW mode is transferred to the flute mode through the nonlinear interaction.

# Nonlinear Energy Transfer



It is considered that the energy of the DW mode is transferred to the flute mode through the nonlinear interaction.

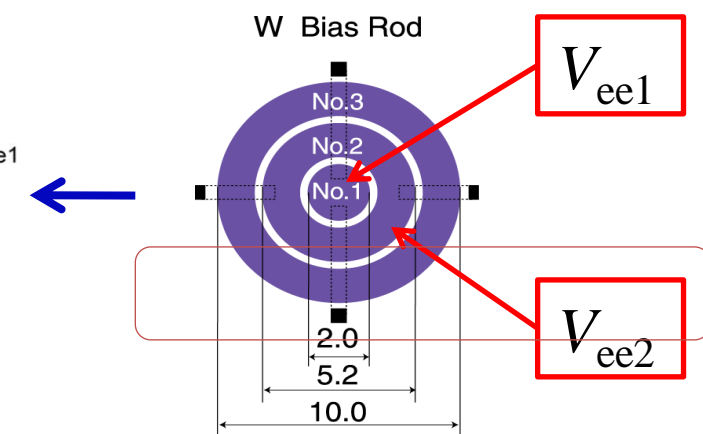
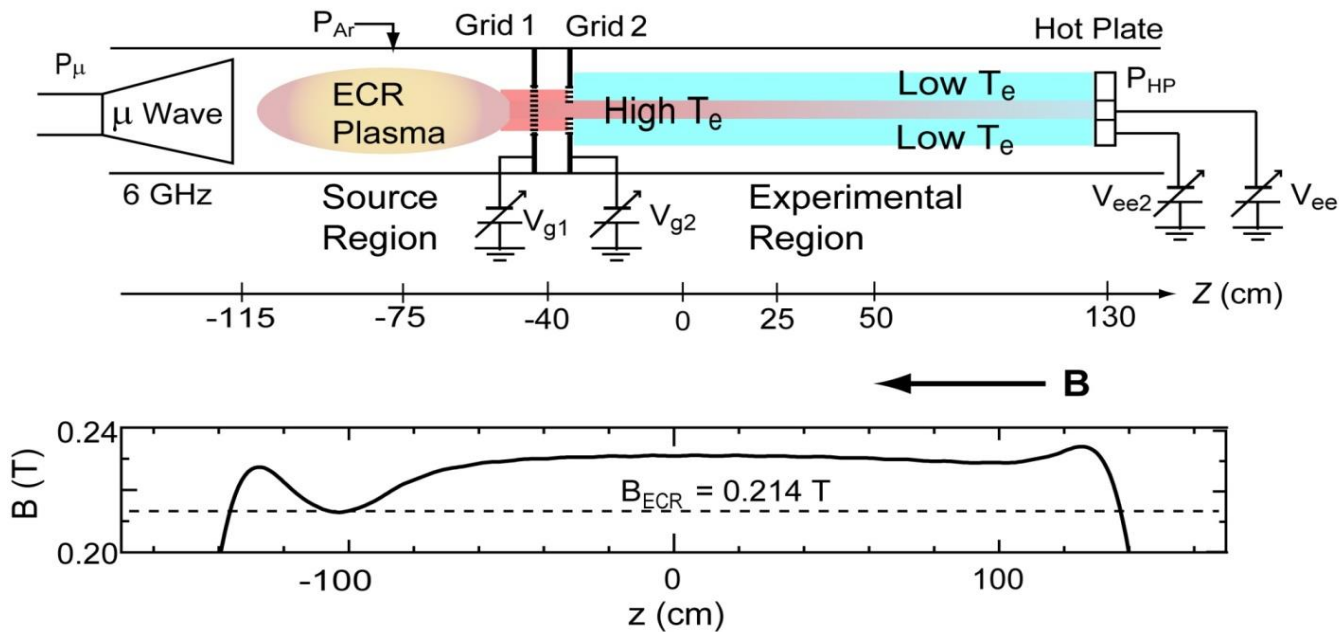
# Nonlinear Energy Transfer



It is considered that the energy of the DW mode is transferred to the flute mode through the nonlinear interaction.

# Effect of $E \times B$ Velocity Shear on ETG mode

45



Electron emitter  
(W hot plate)

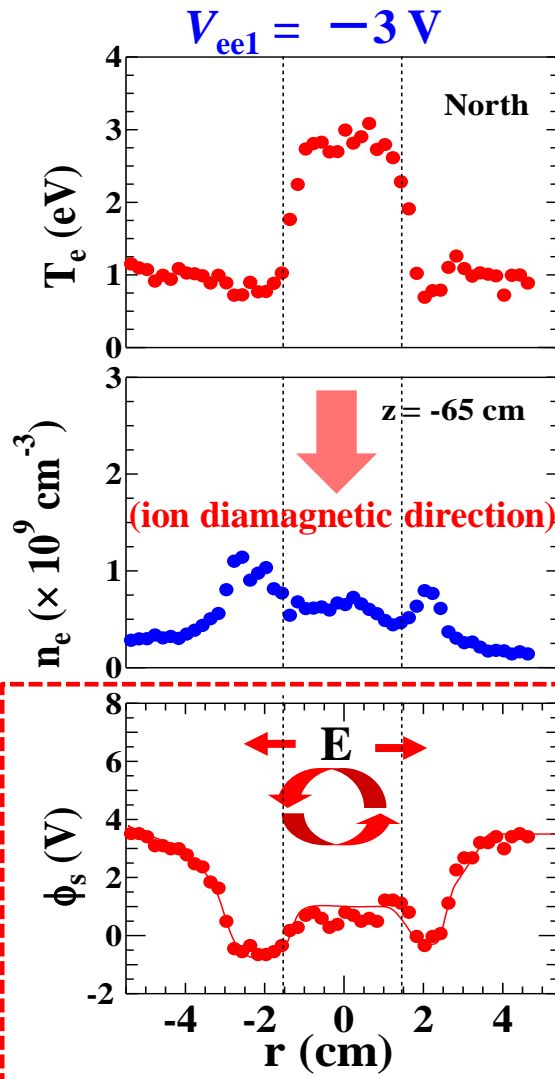
**Q<sub>T</sub> Upgrade Machine**

$$E_r = -\partial\phi(r)/\partial r$$

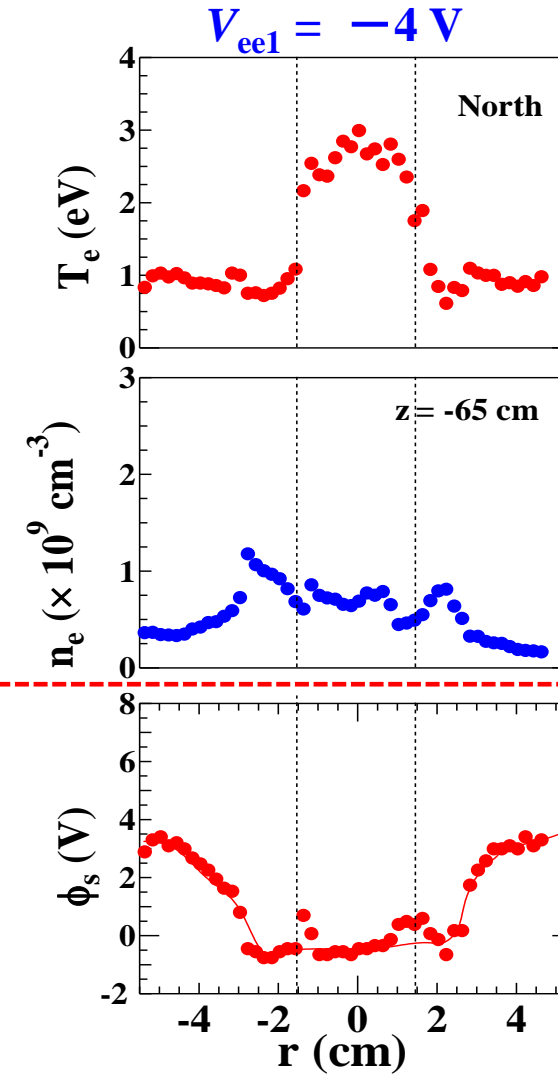
# Control of Radial Electric Field ( $E_r$ )

B  $\otimes$ 

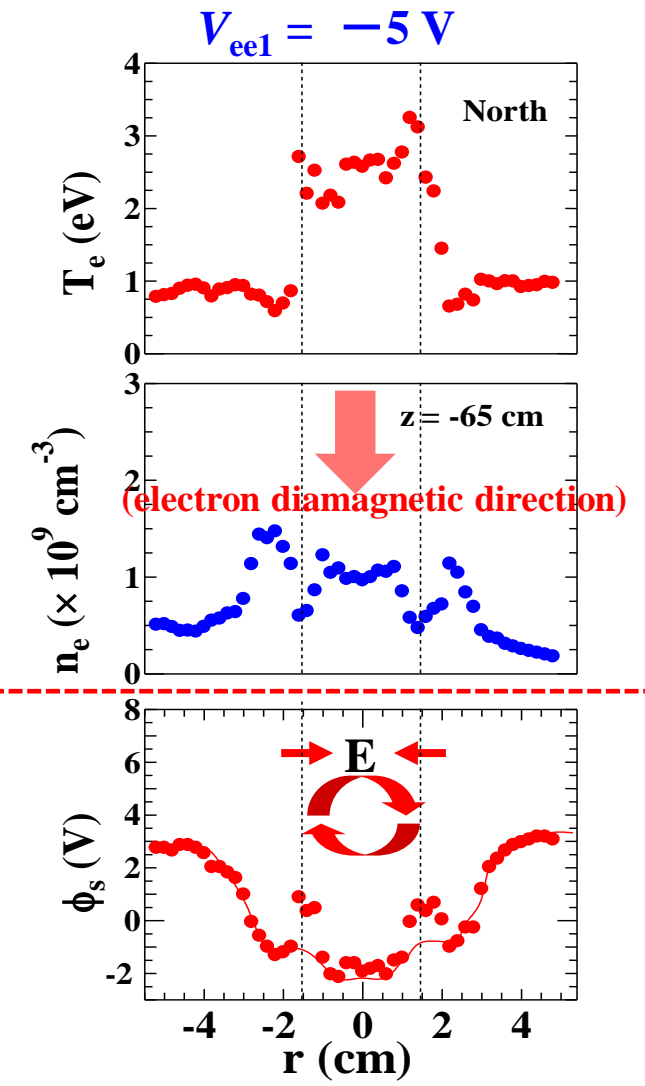
$$P_\mu = 20 \text{ W}, V_{g1} = -10 \text{ V}, V_{g2} = -30 \text{ V}, V_{ee2} = -1.5 \text{ V}$$



$$E_r \approx 1.1 \text{ (V/cm)}$$



$$E_r \approx -0.1 \text{ (V/cm)}$$

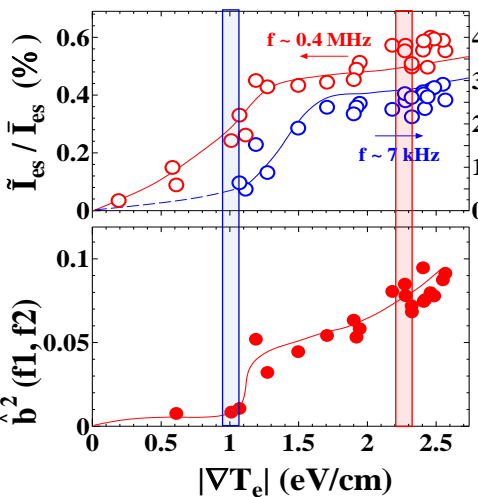


$$E_r \approx -1.0 \text{ (V/cm)}$$

# Effect of the $E_r$ on Fluctuations

$P_\mu = 20 \text{ W}$ ,  $V_{g1} = -10 \text{ V}$ ,  
 $V_{ee2} = -1.5 \text{ V}$ ,  $r = -0.9 \text{ cm}$

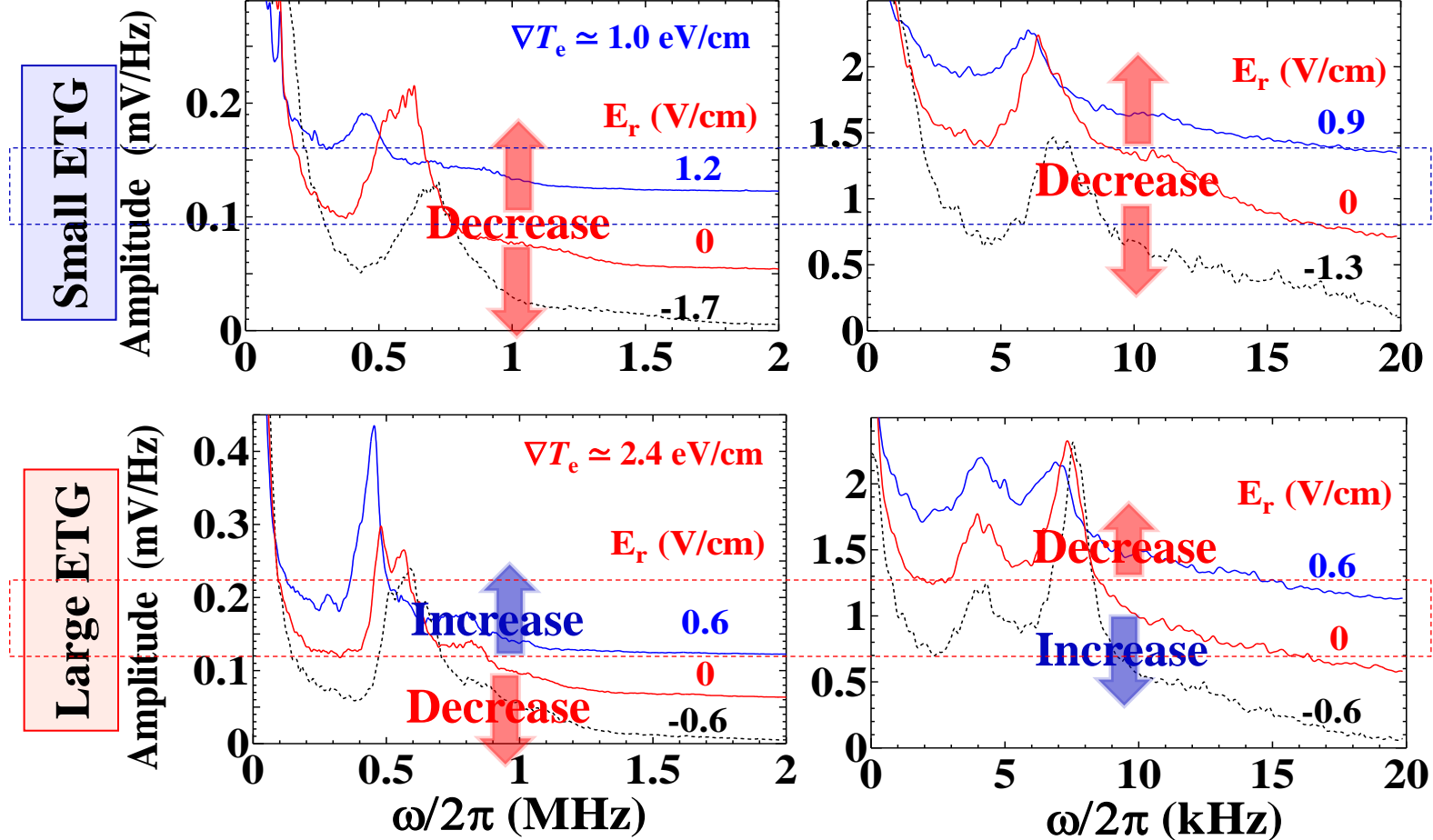
Nonlinear Coupling  
between ETG mode  
and Drift wave mode



Small ETG

ETG mode

Drift wave mode

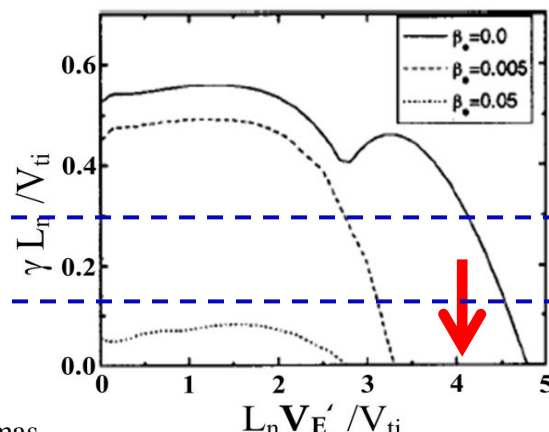


The effect of the  $E_r$  on ETG modes in the large ETG case is certainly different from the small ETG case.

# Effect of the $E_r$ on Fluctuations

## Theories

### ETG mode

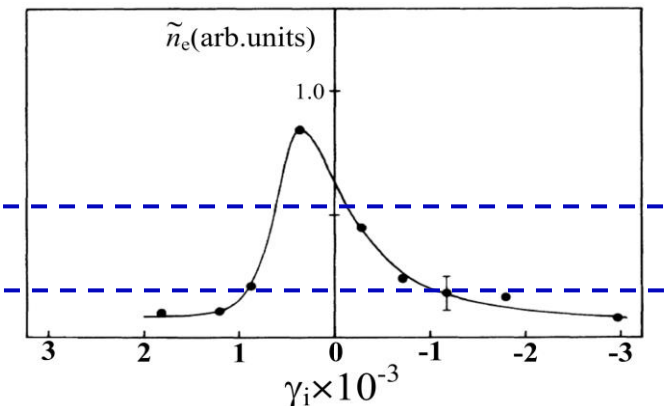


Z. Gao et al., Phys. Plasmas  
11, 3053 (2004).

$V_E'$ : E  $\times$  B Shear Strength

## Experi.

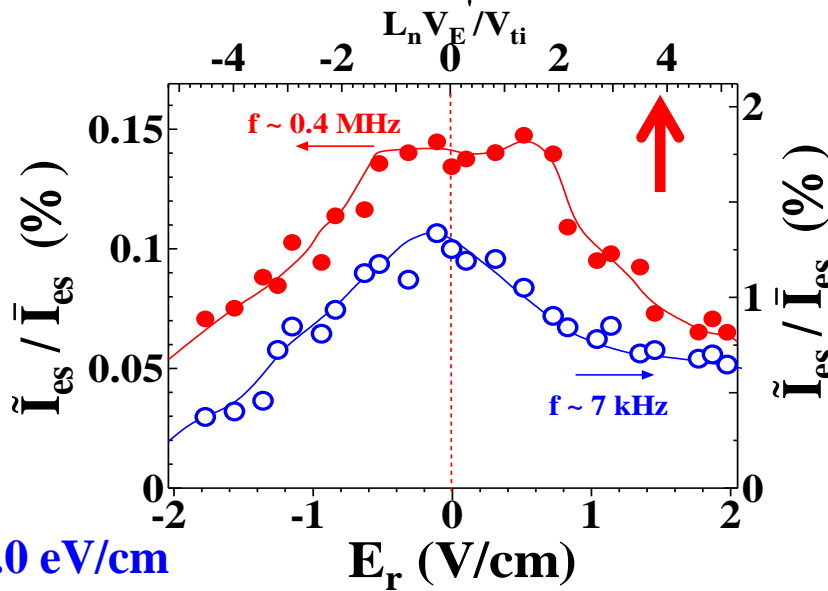
### DW mode



A. Mase et al., Phys. Rev. Lett. 64, 2281 (1990).

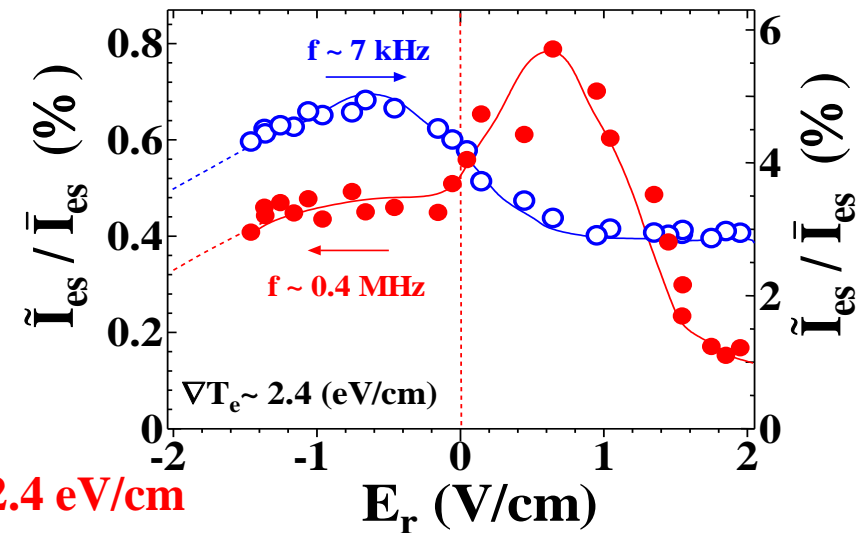
$$\gamma_i \equiv -eE_r/m_i L_\phi \omega_{ce}^2$$

### Small ETG



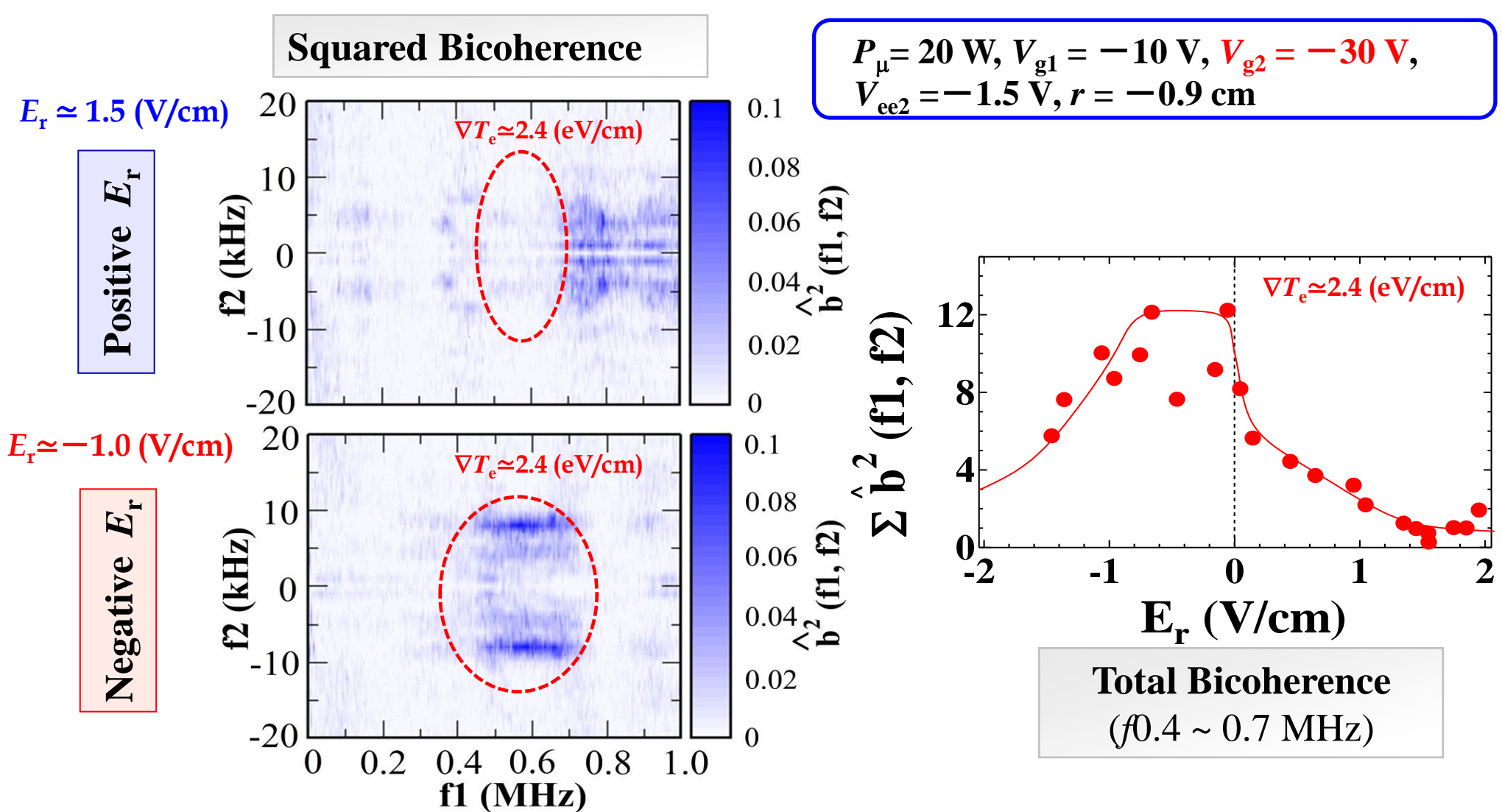
$$\nabla T_e \simeq 1.0 \text{ eV/cm}$$

### Large ETG



The suppression tendency of ETG mode has a significant difference between the slightly negative  $E_r$  and positive  $E_r$  in the large ETG case.

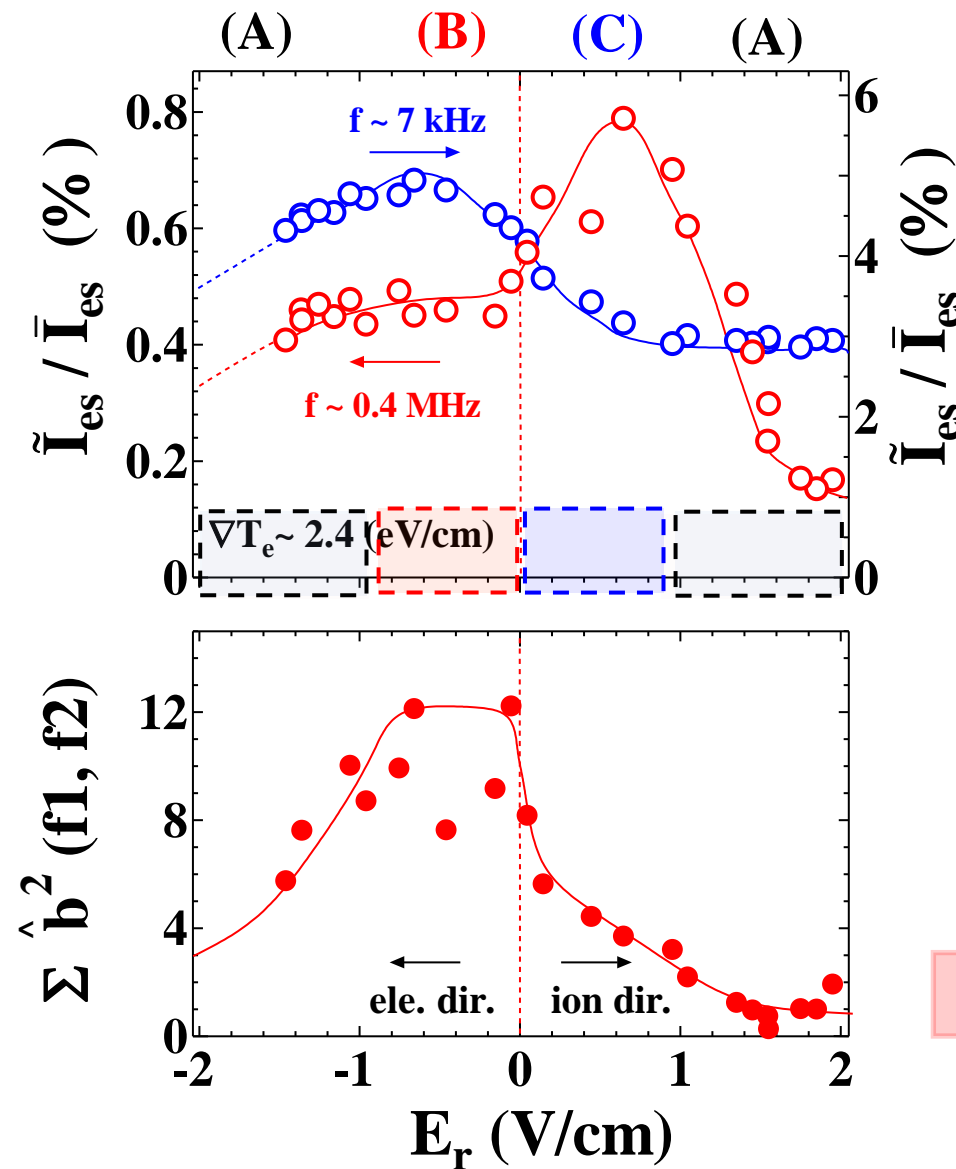
# Dependence of bicoherence on the $E_r$



The nonlinear coupling between the ETG mode and drift wave mode become stronger when  $E_r$  becomes the slightly negative value.

# Effect of $E_r$ on the Nonlinear Interplay

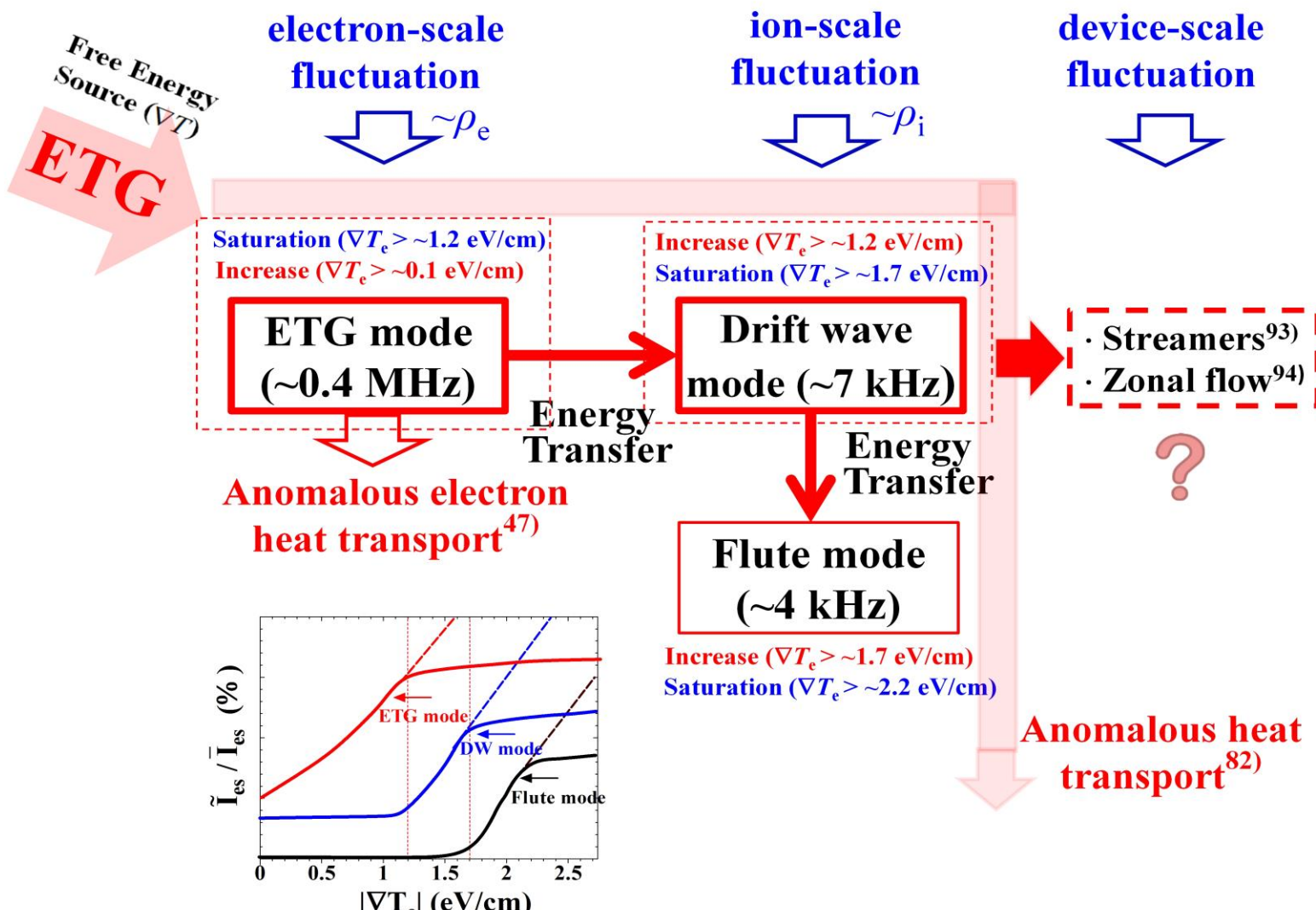
$$P_\mu = 20 \text{ W}, V_{g1} = -10 \text{ V}, V_{g2} = -30 \text{ V}, V_{ee2} = -1.5 \text{ V}, r = -0.9 \text{ cm}$$



- (A) **Suspension of ETG mode**  
=> Owing to the strong  $E_r$   
Effects of  $E \times B$  shear
- (B) **Suspension of ETG mode**  
=> Increasing the Nonlinear Interplay  
=> Increasing the DW mode
- (C) **Sustainment of ETG mode**  
=> Decreasing the Nonlinear Interplay  
=> No energy transfer to the DW mode

The  $E_r$  affects the nonlinear interaction of the ETG and DW modes, which cause the resultant suppression of the ETG mode in the slightly negative  $E_r$

# Effect of ETG on the Nonlinear Interplay



Ref

- 1) F. ...
- 2) C. Moon, et al., Phys. Rev. Lett. **111**, 115001 (2013).
- 3) Y. Nagashima, et al., Phys. Plasmas **16**, 020706 (2009).
- 4) T. Yamada, et al., Phys. Rev. Lett. **105**, 225002 (2010).